Wetland reconstruction by controlling water level in Aamsveen: the effects on variation of vegetation and nutrients

XING LIANGHUI
March, 2015

SUPERVISORS:
Dr. Zoltán Vekerdy
Dr. Christiaan van der Tol
Drs. Eddy.Westinga

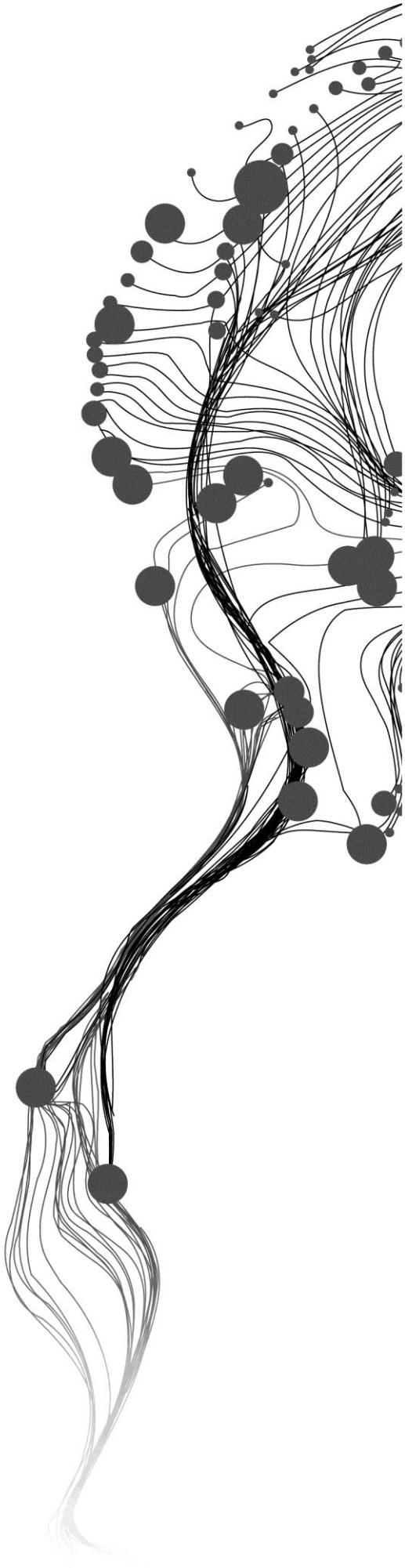

Wetland reconstruction by controlling water level in Aamsveen: the effects on variation of vegetation and nutrients

XING LIANGHUI

Enschede, The Netherlands, February 2015

Thesis submitted to the Faculty of Geo-Information Science and Earth Observation of the University of Twente in partial fulfilment of the requirements for the degree of Master of Science in Geo-information Science and Earth Observation.
Specialization: Water Resources and Environmental Management

THESIS ASSESSMENT BOARD:
Dr. Ir. Mhd S. Salama (Chair)
Ir. Ing. B. van der Worm, Waterschap Vechtstromen
Dr. Z. Vekerdy
Dr. C. van der Tol

ABSTRACT

The wetlands play an important role in the ecosystems because they make the connection between water and land ecosystem. They also are essential to human well-being, and to flora and fauna. Any small change in wetlands may have considerable effects to the ecosystem.

The study area is Aamsveen, a region managed by the Stichting Landschap Overijssel since 1967. The main objective of the research is the re-creation of favourable habitat conditions for the restoration of the native landscape: a raised peat bog. The last significant change in Aamsveen occurred in 2011 when the management closed old tubes and dug a new canal going around the wetland to restore the original steam of the Glanerbeek. Uncertainties regarding the impact of these changes have made it necessary to monitor the changes to groundwater level, vegetation and nutrients.

The targets of this study are to monitor the following: (1) the change condition of groundwater level since 1995; the variation of vegetation between 2002 and 2012; and (3) the new canal's purification capacity for nutrients. For the groundwater Table part, Global Polynomial Interpolation and statistical methods were used to explain the situation of groundwater. For the vegetation part, vegetation detection was produced from official maps of Landschap Overijssel, and remote sensing technology was applied to help us in the analysis of the growth condition of vegetation. For the nutrients part, due to the lack of previous data, field work was taken to measure the water quality of new canal and old canal in autumn.

Key words: Wetlands, Canal change, Vegetation detection, NDVI, GIP, Groundwater level, Water quality

ACKNOWLEDGEMENTS

First of all, I should thank all of the people who always give me help during the study and research in ITC as an MSc.

I would like to extend my utmost gratitude to my supervisors, Dr. Zoltán Vekerdy, Dr. Christiaanvan der Tol, and Drs. Eddy.Westinga. Their encouragements have helped me through the difficult period at the beginning of my research. When I lost my motivation, they reminded me to work hard, and gave me many useful suggestions and critical comments. Without their help and guidance, I wouldn't have been able to finish my thesis.

I acknowledge my father and my mother for all their support, time and trust.

I also thank Dr. Chris Mannaerts, Drs. J.B. (Boudewijn) de Smeth, Bas van der Worm and pHD students, who shared insightful knowledge with me, and help me a lot during the research.

I am also grateful to all my friends and classmates who have helped me in the module study and the research period: Mengxi Yang, Yannan Zhang, Tingting Wei, Yaojun Cao, Xi Zhu, Yifei Xue, Yuangen Jiang, Josip Završki, Badal Kumar Dash, and especially Qibo Li who saved me when we were doing the field work. I wish our friendship will continue, and that everybody can enjoy their life.

TABLE OF CONTENTS

LIST OF FIGURES

LIST OF TABLES

1. INTRODUCTION

1.1. Background

Wetlands cover about 8.5% of the Earth's land surface and include different types of habitats such as permanent and seasonal marshes, fens, peatlands, floodplains, and coastal areas (Jacob er al., 2014). They are among the most important ecosystems on the Earth, they build a connection between water and land ecosystems and provide a wide variety of services and commodities to humanity (Malekmohammadi & Rahimi Blouchi, 2014). They are also considered the most biologically complex of all ecosystems, serving as home to a wide range of plant and animal life.

Peatlands are wetlands consisting of abundant living and dead organic matter. They cover 3% of the Earth's surface. Peatlands are regions that contain a layer of peat on or very close to the surface, which have accumulated naturally over thousands of years. Generally "peatlands" are the wetlands which have common ability to form peat (organic soil produced by the accumulation of plant material). Bogs and fens are two major types of peatlands, both of them occur in similar climatic and geographic regions. Bog is a peatland which receives water solely from rain and (or) snow falling on its surface. Bogs are usually acid areas, frequently surrounding a body of open water (Figure 1.1). Fen is a type of wetland ecosystem characterized by peaty soil, dominated by grass like plants, grasses, sedges, and reeds. Fens are alkaline regions, receiving water mostly from surface and groundwater sources. The difference between the two is based on the hydrological regime: bogs receive water mainly from precipitation, while fens are supplied with water mostly from surface and groundwater sources. When peatlands are abundant, they have an impact on the regional climate, plant species, habitats and water quality around the area.

Any small element change in a wetland may cause turbulence in the ecosystem. For example, in Spain, land-use change became the primary diver behind biodiversity loss, resulting in the conversion of 60% of the original wetland area over fifty years, and 62% decline of ecosystem services (Zorrilla-Miras et al., 2014). Other contributory factors included changes in the groundwater Table, vegetation and nutrients. It is therefore necessary to monitor and map the wetland responses on the change in these factors.

Peatlands are difficult to monitor, especially their inner reaches (Zomer et al., 2009). In-situ data collection is the traditional way to monitor the water quality and vegetation (Siciliano et al., 2008). In the recent years, remote sensing has been shown to be suitable for the study and monitoring of wetland plant communities seasonally and yearly (Martínez-López et al., 2014).

In many Dutch wetlands, surface levels of the surrounding area are up to 1 m lower than the fen reserve. This is caused by water management measures and peat settlement, leading to hydrological changes including groundwater flow alterations. So identifying water Table is critical for analysing vegetation changes in wetland (Lamers et al., 2002). Many hydrogeological applications of remote sensing link image or data interpretation to groundwater processes (Tweed et al., 2006), so it is logical to use this technology in the hydrological assessment of wetlands.

Vegetation growth needs nutrient, so the balances of the nutrient concentrations of the waters entering and leaving the lands have effects on the vegetation types and aquatic ecosystems. The nutrient concentration of water can help vegetation grow well, but high nutrient concentration can reduce aquatic plant growth and reduce species biodiversity of terrestrial vegetation. Furthermore, vegetation types also may influence sedimentation rates of the particles associated to nutrients (Fisher et al., 2009).

Figure 1.1: Pitcture of a bog in Aamsveen

1.2. Study area

Aamsveen (Figure 1.3) is a bog area which is on the Dutch-German border on the south-western side of Enschede. It was formed in the last glacial period of wind-blown sand, covering a low-lying an ice-formed relief (Fassio, 2000). The Dutch part is managed by the Landscape Overijssel since 1967, and it is 145 hectares. This transition area has a wide variety of vegetation types such as bog, bog woodland; wet heath, Nardus grasslands and alder swamp forests. It is formed by about 24.3 hectares of heathland with ponds and marshes; 16.2 hectares of grass. The German part is more than 700 hectares and consists of three parts: the Diskeeper Alstätter Venn and Venn Graeser (Wikipedia, 2014).

Aamsveen is a nature reserve area now, but it was a peat mining area in earlier times, so it has been drained for the mining and also for agriculture and exploitation. Since then, it has been managed by the Stitching Landscape Overijssel, and it has been changed for 4 times with the aim of generating a self-regulated system:

1. In 1969, the last peat extraction took place. For making it possible, a channel was originally dug along the lowest part of the wetland to keep the water level low.

2. In 1983, a plan which aimed to replace the open channel by tubes was carried out. The purpose of that plan was to make the nutrient rich water from the upstream agricultural area flow through the tubes to the Flörbach and from there to the Glanerbeek.

3. From 1993 to 1995, in order to raise the ground water level and reduce the infiltration of nutrient–rich waters coming from the surrounding farmland, the area was divided into smaller compartments with dams.

4. In 2011, the organization closed the tubes and dug a new channel (Figure 1.2.b) which goes around the wetland to restore the original stream of the Glanerbeek (Figure 1.2.a). So from that moment, the water flows around the wetland to the Glanerbeek again. According to the plans, the canal with the tube doesn't drain the bog-area anymore.

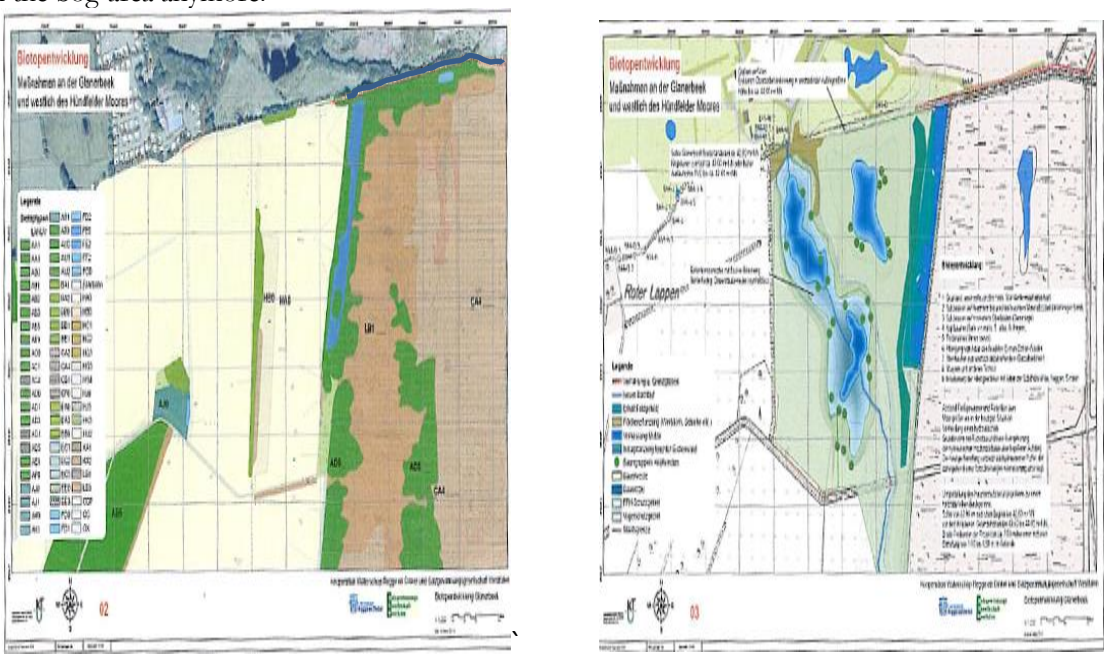

(a) (b)

Figure 1.2: The area upstream from the wetland (a) before the canalsion; (b) after the canalsion

Figure 1.3 The whole area of Aamsveen. The red line is the old channel with the tube, the tube followed the border from the purple line; the purple lines show the old system at the area where the canal was later installed and the blue lines show the new canal channel dug in 2011.

1.3. Research problem

In this wetland area, a project had been implemented to reconstruct the natural state of the bog. After the channel changes, this project has effects on the hydrology of the wetland, which is expressed in water cover and some vegetation changes. If we want to know the efficiency of this project, it's necessary to understand how the peatland water level changed and how it affected the land cover of the wetland in the last 15 years by comparing the older states with the recent situation. Furthermore, the whole area needs very detailed monitoring, for which the recently operational satellite sensors provide limited possibilities. An optimal monitoring method needs to be worked out.

1.4. Objectives

1.4.1. General objective

This study aims to analyse the effect of altering the course of the draining canal in the Aamsveen on the vegetation and water cover by combining field and remote sensing techniques.

1.4.2. Specific objectives

In order to achieve the main research objective the following specific objectives are set for the study:
1. To make wetland vegetation variation maps with the existing official maps (Landschap Overijssel); and calculate NDVI between 2002 and 2012;
2. To analyse the changes of groundwater levels in the last 20 years;
3. To analyse the spatial distribution of the nutrients in the wetland;
4. To find the relationship between the groundwater levels, wetland cover changes, groundwater level;
5. To define the accuracies and limitations of the used techniques for wetland monitoring;

1.5. Research problem

The following research questions are to be answered to achieve specific objectives of the research:
1a. How to map the surface cover with the available remote sensing data?
1b. How can we quantify changes in time with optical remote sensing methods?
2. How did the groundwater regime change in the last fifteen years?
3. Is there a spatial pattern of nutrient concentrations in the wetland?
4a. How have the water cover, the vegetation and the groundwater changed in the last fifteen years?
4b. Is there a relationship between the (ground) water level changes and the wetland cover changes?
5. Is the information provided by the applied methods sufficient for wetland management?

2. LITERATURE REVIEW

This section briefly describes the satellite remote sensing of wetlands, and methods to identify and separate the land cover types.

2.1. Previous work on Aamsveen

In 2000, a study was conducted to monitor the vegetation changes between 1984 and 1998, with particular attention to the hydrologic conditions and to indicator species by remote sensing technologies (Fassio, 2000). The studied period included the three years when the area was subdivided into smaller compartments with dams (1993 to 1995).

The author found that *Molinia* and *Molinia* + *Pteridium* occupied the largest areas in the two maps marking the beginning and the end of the studied period. Half of the area changed; some of the changes were probably caused by the dams. Also, a report (Gutierres, 2012) in 2012 mentioned the Aamsveen nature 2000 site. It was depended on the principle of ecological indication. The field observations were based on biotic, abiotic, structural and spatial characteristics in order to assess. The researcher used the vegetation indication to assess the effects caused by the dams. It shows the management of Aamsveen was successful, because the groundwater level in the area raised and the restoration of the wet meadows was on the way. At the same time, many plants and animals have come back to the place (Gutierres, 2012).

2.2. Review on satellites

As the techniques of satellite remote sensing developed, it has been used to study all types of wetlands and to map large wetland ecosystem (Ozesmi & Bauer, 2002). The multi-temporal imagery is often very helpful in classification of wetlands. For example, wetlands in the St. Johns River Water Management District of Alachua County, Florida were analysed using image segmentation of Landsat 7 imagery, and the mapping accuracies were more than 88% (Frohn et al., 2009). In a case in Elkhorn Slough, central California the nutrient enrichment was evaluated by hyperspectral imaging of wetland vegetation (Siciliano et al., 2008). A further example is a study of the material and energy fluxes in a wetland was studied with the help of Landsat 5 satellite data (Loiselle et al., 2001).

Although high spatial resolution remote sensing can provide high-resolution maps, it has a higher price and provides lower spectral and temporal resolution. The lower temporal resolution makes it impossible to produce time series analysis with one satellite (Dams et al., 2013). In many cases, aerial photography is more suitable for detailed mapping of wetland. In addition, the water levels/cover and land cover changes in wetlands can be also monitored by combining aerial photography and satellite remote sensing data together (Ozesmi & Bauer, 2002).

Landsat 5 TM, SPOT-5, and ASTER are satellite remote sensing systems that have been used to study wetland and land surface cover. Table 2.1 compares the characteristics of these sensors.

Depending on the small area of Aamsveen and financial reason, ASTER sensor is suitable for my study. It was built in a collaboration of NASA and the Japanese Ministry of Economy, Trade, and Industry (METI)(The Yale Center for Earth, 2010).Land surface temperature, emissivity, reflectance, and elevation data can be acquired by ASTER. It has 3 visible and 11 in the infrared region of the electromagnetic spectrum (Table 2.2). Band 3 has a nadir and backward facing which gives it the unique ability to create digital elevation models based on stereo images. The revisit time of it is 16 days which can be a limitation for studying rapidly changing surface conditions. The area of an ASTER scene is 60 km by 60 km., Data is collected simultaneously at three resolutions. There are several ASTER products derived from the data.

Unique scaling is needed for each band for the calibration. ASTER L1B Registered Radiance at the Sensor product is the primary full ASTER dataset which has 16 bands of data. The data of ASTER can be downloaded from the USGS website.

Table 2.1: Comparison of Landsat 5 TM, SPOT-5, ASTER remote sensing data

	Landsat 5 TM	SPOT-5	ASTER
Number of bands	7	6	14
Radiometric (bits)	8	8	8
Temporal resolution	16 days	3 days	16days
Spatial resolution (MS)	30 m	10 m	15 m
First launched	1982	2002	1999

Table 2.2: ASTER Band Details

Band	Label	Wavelength	Resolution	File Number
B1	VNIR_Band 1	0.52 – 0.60	15m	First File
B2	VNIR_Band 2	0.63 – 0.69	15m	
B3	VNIR_Band 3N	0.76 – 0.86	15m – Nadir view	
B4	VNIR_Band 3B	0.76 – 0.86	15m – Backwards scan	Second File
B5	SWIR_Band 4	1.60 – 1.70	30m	Third file
B6	SWIR_Band 5	2.145 – 2.185	30m	
B7	SWIR_Band 6	2.185 – 2.225	30m	
B8	SWIR_Band 7	2.235 – 2.285	30m	
B9	SWIR_Band 8	2.295 – 2.365	30m	
B10	SWIR_Band 9	2.36 – 2.43	30m	
B11	TIR_Band 10	8.125 – 8.475	90m	Fourth File
B12	TIR_Band 11	8.475 – 8.835	90m	
B13	TIR_Band 12	8.925 – 9.275	90m	
B14	TIR_Band 13	10.25 – 10.95	90m	
B15	TIR_Band 14	10.95 – 11.65	90m	

2.3. Atmospheric correction

Atmosphere correction is a very important pre-processing step to get high quality data in many remote sensing applications. Because the study area have digital number (DN) values which can't be calculate directly, and the contents of aerosol or water vapour in atmospheric can affect satellite sensor to acquire the real reflectance of land surface because of the changing of the top of atmosphere (TOA) radiance. At the same time, the Solar Zenith Angle (SZA) and the View Zenith Angle (VZA) also influence in determining the effects of the atmosphere. So an atmosphere correction scheme aims to exclude the effects by atmosphere. It modifies the TOA radiance measurement recorded by a sensor in conformity to calculate values for the atmospheric absorption and scattering along the path travelled by incident light (Proud et al., 2010). There are several methods that frequently used to do atmosphere correction, like 6S, FLAASH, or SMAC.

FLAASH (Fast Line-of-Sight Atmospheric Analysis of Spectral Hypercubes) model is a keystone of atmospheric correction, but it is only applicable to bands between 0.35μm to 2.5 μm (The Yale Center for Earth, 2010).

6S is the abbreviation of the Second Simulation of the Satellite Signal in the Solar Spectrum which is improved version of 5S (Simulation of the Satellite Signal in the Solar Spectrum)(Vermote, Tanré, Deuzé,

Herman, & Morcrette, 1997). Kotchenova & Vermote (2007) shows the validation process for 6S and the results proved that the 6S scheme can be used to get high accuracy in most situations.

The Simplified Method for Atmosphere Correction (SMAC) is a simplified method, parameterized by the 6S. It reduced complexity and enables the atmospheric correction to be quickly performed on a large data set. It is more simplified than 6S, and a number of the complex components that are modelled with 6S are not included in the SMAC. Therefore SMAC works 3000 times faster than SMAC and with proper atmospheric data, the accuracy is within 2-3 percent in comparison to 6S (Proud et al., 2010). The SMAC is free and open source, so it's very convenience to use.

2.4. NDVI

There are many methods to map the vegetation changes. They can be divided into two main types: one uses vegetation indices; the other uses classification techniques.

The vegetation indices can be used to map wetlands and other land cover types with remote sensing methods. It is sensitive for both spatial and temporal variations in vegetation photosynthetic activity and canopy structural variations. The normalized difference vegetation index (NDVI) is a normalized ratio of NIR and red bands (Huete et al., 2002). It's not very sensitive in high density areas, so some other indices were developed, e.g., the enhanced vegetation index (EVI). NDVI is sensitive to chlorophyll, but the EVI is more responsive to canopy structural variations. They are leaf area index, canopy type, plant physiognomy, and canopy architecture(Gao, Huete, Ni, & Miura, 2000).Huete et al. (2002) found that NDVI is sensitive in high biomass region, e.g. in the Amazon, while the EVI is sensitive to canopy variations.

Classification techniques are dependent on different spectral responses of wetland vegetation types. So it's useful to know which wetlands vegetation types are spectrally separable and which bands are best for wetland discrimination. Classification methods can be described in three categories: unsupervised, supervised, and hybrid approaches. The easiest to apply is unsupervised classification, but in supervised classification the operator can have more control over the resulting classes. For example to the latter, Shanmugam et al. (2006) compared the recently evolved soft classification methods based on linear spectral mixture modelling based on the interactive self-organizing data analysis (ISODATA) and maximum likelihood classification (MLC) algorithms to. They found that MLC classification method produced maps with higher accuracy than ISODATA classification method.

But for my study, due to the limitation of remote sensing data, the classification is not suiTable for researching, so NDVI was used to analysis the vegetation.

2.5. Interpolation methods

Interpolation is a way to construct new data points with the range of a discrete set of known data points("Interpolation - Wikipedia, the free encyclopedia,"). For environmental analysis, the data is collected in fixed stations, which is spread over a geographic region. But researchers need some information about some others locations or (and) regions not included by the monitoring stations to do analysis, plan and decision. These interpolation models aim to a predictions for the unmeasured areas. And geographic information system (GIS) is a helpful tool to interpolate climatological and metrological information. Furthermore, interpolation shows very good prospects for water quality and water level mapping (Bajjali, 2012)(Gundogdu & Guney, 2007). The geostatistical methods of Global Polynomial Interpolation (GPI), Inverse Distance Weighting (IDW), and Kriging are often used for interpolation.

Water level is a non-stationary variable, so each data set can fit different models because of the different spatial structures. A GPI map represents a whole area with a single spatial function based on an entire dataset. The surface can be modelled with a linear or more complex trend surface, where linear trends

describe only the major direction and rate of change; while the trend surfaces explained with polynomials of higher orders provide progressively more sophisticated descriptions of spatial patterns (Bajjali, 2005).

In the IDW method, the weighted average is decided by the distance between neighbouring points. The important difference to the nearest neighbour approach is that it considers the distance between more observations not only two. The method produces better results in interpolating climate data (Sluiter, 2009).

Kriging provides an estimate of the error and uncertainty of the prediction additionally to the interpolated values. Optimal weights are distributed to the measured values to calculate the unknown ones. Because the variogam changes with distance, the weights depend on the known sample distribution (Bajjali, 2012).
Oasmaa, Elliott, & Mu (2009) made the comparison of 10 commonly used interpolation methods and their applications. They point out that GPI is suitable for the region having sparse data and with the increasing complexity of the method, the estimation errors will increase; although IDW is easy to use, spatial arrangement of samples doesn't affect weights; while Kriging is best to calculate with well-distributed data.

2.6. Statistics methods apply in hydrology

Statistics is a method of mathematics to study the collection, analysis, interpretation presentation, and organization of data. Statistical techniques have been widely applied in many domains, such as medicine science, behavioural sciences, chemistry and biology which often get accurate results. For example, Katz, Parlange, & Naveau (2002) proved that the statistical approach to extremes play an important role in engineering practice for water resource design and management. Statistical techniques had been used to map sea level pressure (SLP)and sea surface temperature SST and to forecast cold/warm season air temperature over the United States (Barnett & Preisendorfer, 1987).

There are statistical methods to analyse the relationship of groundwater level, precipitation, evaporation, and flow, like multivariable statistical analysis and correlation analysis.

The correlation methods can be divided into three groups: bivariate, partial, distance. The simplest way to see the relationship between two datasets is to calculate the correlation coefficient. A bivariate correlation is a correlation between two variables which can be realized by Pearson's product-moment correlation coefficient, Spearman's rho, and Kendall's rank correlation coefficients in the SPSS (Statistical Package for Social Sciences) software (Field, Miles, & Field, 2012). Pearson product-moment correlation coefficient or Pearson correlation coefficient, r, is used to describe the direction and degree to which one variable is linearly related to another. Spearman's correlation coefficient, ρ, is a non- parametric statistic and can be used when the data violates parametric assumptions such as normal distribution. Kendall, τ, is a non-parametric correlation coefficient that is good to be used to assess and test correlations between non-interval scaled ordinal variables (Bolboaca & Jäntschi, 2006). Spearman correlation coefficient was used in groundwater level to investigate whether the groundwater levels which had different distances from a stream in the upslope were common hydrological pattern (Seibert, Bishop, Rodhe, & McDonnell, 2003).

For describing how significant the correlation is, the t-test is a versatile statistical method. It can be used to test whether a correlation coefficient is different from 0, or a regression coefficient, b, is different from 0, or whether two group means are different.

2.7. Water quality

All living beings need nutrients, nitrogen (N) and phosphorus (P) to exist. At the same time, they also can damage creatures if they are in excess. Nutrient enrichment is a major concern in many wetlands which play vital ecosystem roles in water quality improvements (Fisher et al., 2009). Water quality is impaired by the nonpoint source pollution from the surrounding around area (C.-Y. Wang, Sample, Day, & Grizzard, 2014). One of some artificial and natural wetland functions is the removal of pollutants from runoff.

Unfortunately, few studies have focused upon the nutrient distribution in wetlands (C.-Y. Wang et al., 2014). So some researchers (C.-Y. Wang et al., 2014) tried to grow different plants in a nutrient enriched urban wet pond to study vegetation biomass and phosphorus (P) distribution. This study proved that above-ground plant harvest (especially pickerelweed) can contribute to (P) removal. An investigation made by Fisher (2009) and his colleague shows the variation in nutrient removal in three different wetlands with different vegetation compositions, inflow nutrient concentrations and hydraulic loadings. The results show that the nitrate, orthophosphate and total phosphorus could not be removed over the research year at the same time. For example, the beds with Iris and mixed vegetation could remove ammonium (NH_4) but increased nitrate concentrations in the meantime.

Fast, efficient, and synoptic methods are needed to monitor and detect nutrients in wetlands and coastal systems by at multiple spatial and temporal scales Siciliano (2008) used HyMap hyperspectral imagery and long-term in situ data to extract the nitrogen from a shallow and long (11.5 km) river which crosses the Monterey Bay National Marine Sanctuary.

3. METHODOLOGY AND DATA

Aamsveen is a relatively small area, so only remote sensing of high spatial resolution can be used. The area of open water bodies is also small, so the water quality samples were taken only from the old channel and the new channel.

3.1. Methodology overview

Detailed and long-term monitoring is required to analyse the vegetation changes in wetlands. Thus, over a time period of 12 years (2002-2014), ASTER images were used to calculate NDVI.

For defining vegetation changes, two existing vegetation type maps were compared in this study.

Five steps were followed:
Step 0: Collection of satellite images maps, aerial photographs and groundwater in situ data.

Step 1: Performing atmospheric correction on ASTER satellite images over the Aamsveen wetland with the SMAC Model. NDVI was used to monitor the plants' growing stage. Re-classification of the vegetation maps to a common legend

Step 2: Making the groundwater level maps of the Aamsveen wetland with the Global Polynomial Interpolation Model, based on the time series of the groundwater wells.

Step 3: Combining the vegetation maps and groundwater maps statistically to analyse the possible relationship between the two.

Step 4: Nutrient analysis: Water samples were taken in the inflow and outflow area and at selected points inside the wetland for nutrient content analysis. The following parameters were defined: nitrate, nitrite, total nitrogen, phosphate, pH and temperature. Then the nutrient distribution map was compared with the wetland cover and the groundwater depth maps.

Step 5: Assessment of the relationship between the wetland cover and the groundwater and the analysis of the nutrient distribution.

The flow chart of the study is shown in Figure 3.1.

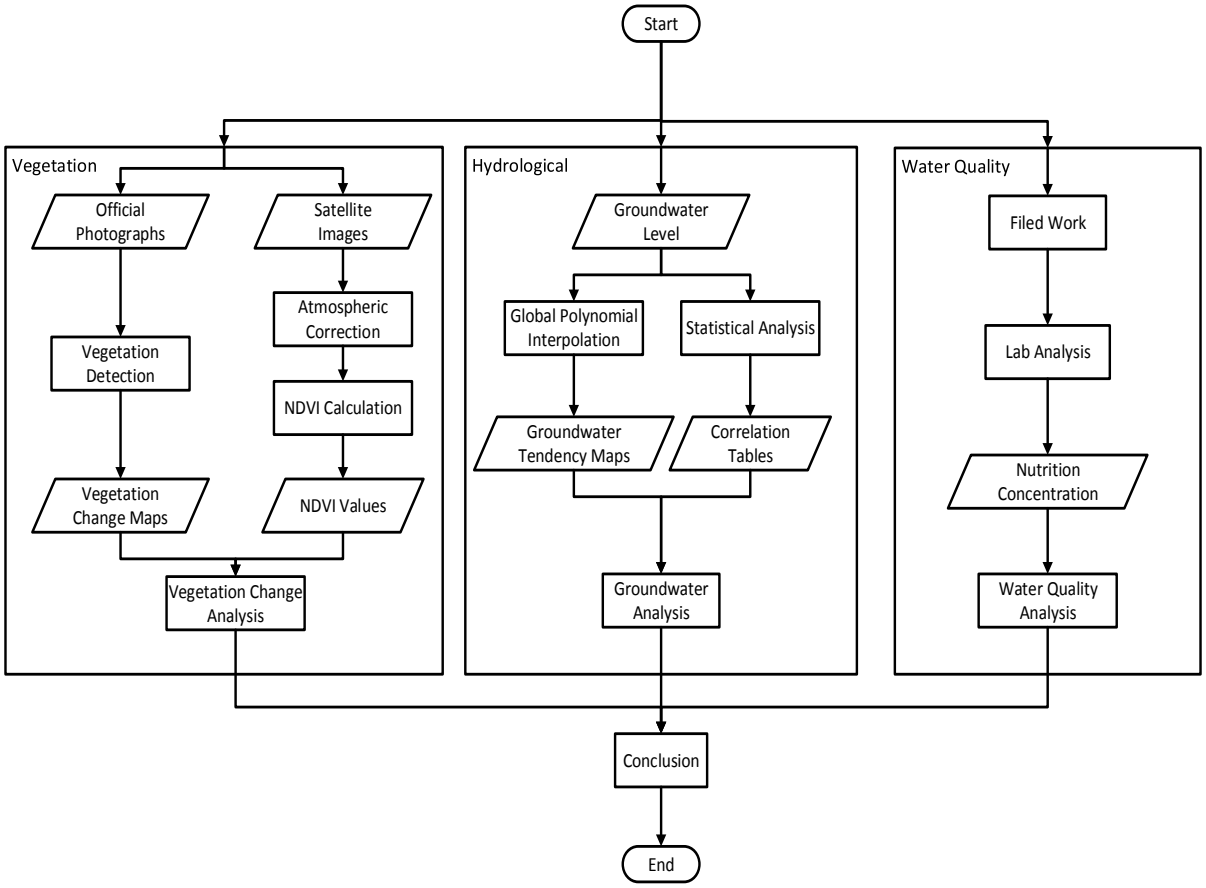

Figure 3.1: Flow chart of Methdology

3.2. Available data

For the reliability of the study, it is necessary to explain the data resources:

1. Satellite images

Based on the study area's properties, the ASTER satellite images are suitable for this research. ASTER satellites have relatively high resolution, and equipped with 14 bands which can provide much information about the surface. There are only 13 usable satellite images provided by USGS from 2000. Due to the NDVI is affect by the temperature and seasons (J. Wang, Rich, & Price, 2003), it's better to choose the data in same month. The data in April were used to calculate the NDVI. They are 15 April 2004 and 20 April 2014.

2. Vegetation maps

The vegetation maps which were used to analyse the vegetation change are made available by Landschap Overijssel (Figure 3.2). The scale of vegetation map in 2002 is 1:5000. It has 9 big categories, and the vegetation map in 2012 which has the same scale of the other map has 26 big categories. So the vegetation map in 2012 has much more details than the map in 2002. The codes for the vegetation type in 2002 and 2012 can be found in appendix A and B.

3. Groundwater data

The data of groundwater, rainfall and evaporation can be downloaded from websites. The data of groundwater level was downloaded from DINOloket (https://www.dinoloket.nl/), and the data of rainfall and evaporation came from Koninklijk Nederlands Meteorologisch Instituut (KNMI) (http://www.knmi.nl/klimatologie/daggegevens/download.html). Most of the groundwater data are available from 1994 and 1995 to the end of 2013, but the sampling frequency is not uniform, the gaps vary generally from 5 days to 20 days. The rainfall and evaporation data was provided with a daily frequency.

4. Water quality data

Nutrient concentrations were obtained from field work. There are 12 sample locations to measure the water quality. The times of the measurement are 23 Oct, 8 Nov, and 22 Nov with Horiba U10 and HACH spectrophotometer.

(a)

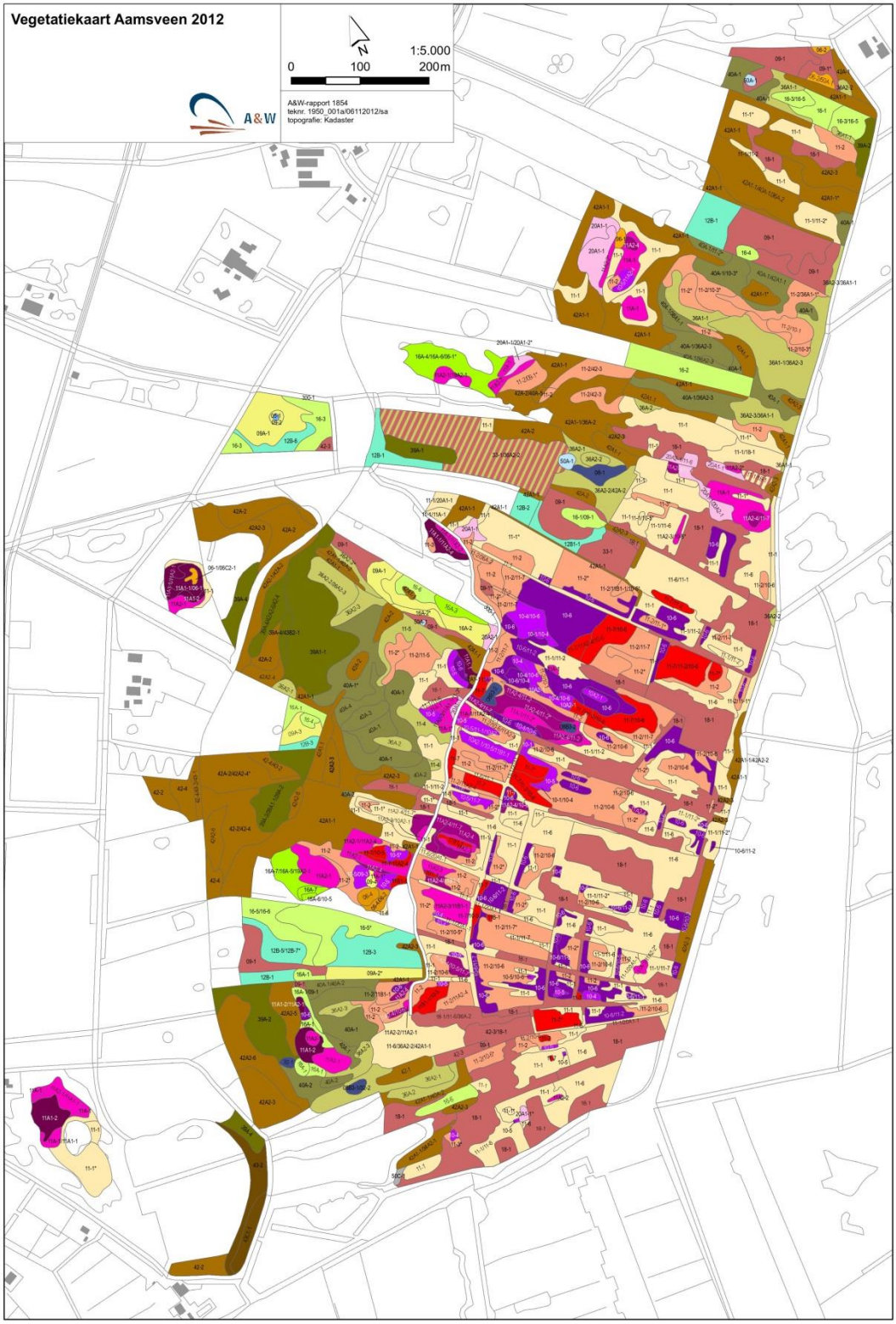

(b)

Figure 3.2: Original vegetation maps made by Landschap Overijssel (a) vegetation types in 2002 (b) vegetation types in 2012.

3.3. Vegetation analysis with NDVI

3.3.1. Atmospheric correction

In the first step, it is necessary to convert the spectral data given in digital numbers (DN) to radiance units with Eq.(3.1)(Finn, Reed, & Yamamoto, 2012).

From digital number to radiance (The Yale Center for Earth, 2010)

L_λ = 'gain' * DN + 'offset' (3.1)

Where: L_λ is Spectral Radiance at the sensor aperture in W / (m^2 * sr * μm). Value range: 0-400.
'gain' is a rescaling factor (can often be found in the header or ancillary data record)
'offset' is a constant

ASTER gain is determined from the header file
In this case, band 2 and band 3N are needed to calculate NDVI. For 2, high gain (0.708) was used in that formula; normal gain (0.862) was used for band 3N.

Table 3.1: Gain value for band 1,2,3, and 3N

Band No.	Coefficient (W/(m^2*sr*μm)		
	High gain	Normal gain	Low gain 1
1	0.676	1.688	2.25
2	0.708	1.415	1.89
3N	0.423	0.862	1.15
3B	0.423	0.862	1.15

Then the radiance was transformed to reflectance by the Eq.(3.2):

$$\rho_p = \frac{\pi * L_\lambda * d^2}{ESUN_\lambda * \cos\theta_S} \quad (3.2)$$

where:
ρ_p is unitless planetary reflectance (values: 0-1)
L_λ is spectral radiance at the sensor's aperture in W m^{-2} sr^{-1} μm^{-1}. Value range: 0-400
d is Earth-Sun distance in astronomical units
$ESUN_\lambda$ is mean solar exoatmospheric irradiances in W m^{-2}
θ_S is solar zenith angle in degrees

The Earth–Sun distance depends on the calendar date of the scene that is expressed in Julian days. The solar zenith angle is included in the header file by the data provider.

The SMAC algorithm uses a set of relatively simple Equation (Eq.3.3) to minimise the effects of the atmosphere and compute the land surface reflectance. As such, 7 input variables are required to be specified: Solar Zenith Angle (SZA, θ_s), View Zenith Angle (VZA, θ_v), Relative Azimuth Angle (RAA, ϕ_r), aerosol optical depth (AOD) at 550 nm (τ_{550}), water vapour content of the atmosphere (uWV) and the ozone content of the atmosphere (uO_3). This input can be derived from websites.

$$\rho_{sat} = \tau_{abs} * \left\{ \rho_a + \tau(\theta_s) * \frac{\rho}{1-\rho*\rho_a'} * \tau(\theta_v) \right\} \quad (3.3)$$

where :
ρ_{sat} is surface reflectance;
τ_{abs} is the gaseous transmittance of the atmosphere;
$\tau(\theta_v)$ is the total upward atmospheric transmittance;
$\tau(\theta_s)$ is total downward atmospheric transmittance;
ρ is the albedo of the land surface;

ρ_a is the reflectance of atmospheric;
Header file for each ASTER image includes the solar azimuth angle, solar zenith angle. Other information can be search on the internet: the data of AOD and water vapour for each measure day were downloaded from AERONET (AErosol RObotic NETwork), which provides globally distributed observations of AOD, inversion products, and perceptible water in canalse aerosol regimes. The network is established by NASA and pHOTONS (http://aeronet.gsfc.nasa.gov/).

3.3.2. NDVI

The Normalized Difference Vegetation Index (NDVI) was used for monitoring the Aamsveen wetland. It's calculated by the reflectance in the near infrared (NIR) and red spectral bans (Equation 3.4):

$$NDVI = \frac{NIR\ band - Red\ Band}{NIR\ band + Red\ Band} \quad (3.4)$$

For the ASTER satellite, band 2 is the NIR band and band 3 is the Red Band.

Since the official vegetation maps were made in 2002 and 2012, so the best matching ASTER data of the available data set, i.e. the images acquired on 15 April 2004 and 20 April 2014 were selected to make a comparison by the Equation 3.5:

NDVI_difference= NDVI_2014 – NDVI_2004 (3.5)

3.4. Vegetation change mapping

All available data was in digital form and pre-processed for placing them into GIS to perform analysis. Due to a slightly different mapping approach, the map made in 2012 (scale 1:5000) have more details than the map made in 2002 (scale 1:5000). A re-classification was carried out based on the map of 2002, to facilitate the comparison. Here are the specific steps:

1. The digital data were resampled into a common geometric frame with rectification. The geometric characteristics of the pixels were made identical to compare the land cover.

The two maps had different vegetation type classification schemes. In order to compare them, they were both generalized to the categories of vegetation structure types. These were: open water, bog, marsh, heath, high tall herbs, pioneer forest, grassland and agriculture field.

2. The maps of vegetation structures in both years were combined into one layer using the Intersect function in ArcGIS. Two types of combination have been made; one is 'no change map', the other one is 'change details map'.

3.5. Hydrological Analysis of the Aamsveen

3.5.1. Global polynomial interpolation

In order to observe the groundwater-Table, monthly data of observation well were used. As it was previously described, GPI captures coarse-scale patterns in the data by fitting a polynomial. A first-order global polynomial fits a single plane through the data. A second-order global polynomial fits a surface with a bend in it, allowing surfaces representing valleys. A third-order global polynomial allows for two bends; and so forth. However, usually a single global polynomial does not fit the data perfectly. In the case of the Aamsveen, there are only 11 groundwater level observation wells available. This setup is not sufficient to show the minor variations in the groundwater Table, so a first-order global polynomial and a second-order global polynomial were used to assess the trends of the wetland's groundwater Table.

3.5.2. Correlation analysis and T – test

The first step was to analyse the relationship between groundwater and precipitation, evaporation and flow. As the properties are mentioned in chapter 2.6, Spearman's correlation coefficient is a non-parametric statistic, and it is not necessary to make any assumption about the frequency distribution of the variables. The data of There are two methods to calculate Spearman's rank-order correlation which explained with Equation3.6 and Equation 3 (SD Bolboaca, 2006).

$$\rho = \frac{\sum_i (x_i - \overline{x})(y_i - \overline{y})}{\sqrt{\sum_i (x_i - \overline{x})^2 \sum_i (y_i - \overline{y})^2}} \tag{3.6}$$

where:
ρ is the Spearman's rank correlation coefficient;
x_i is the rank of the measured groundwater level;
$\overline{x}$ is the average of groundwater level;
y_i is the rank of precipitation, evaporation, precipitation-evaporation and flow;
$\overline{y}$ is the average of precipitation, evaporation, precipitation-evaporation and flow.

The simple formula for ϱ is based on the difference between each pairs of rank (Equation 3.7)

$$\rho = 1 - \frac{6 \sum {d_i}^2}{n(n^2 - 1)} \tag{3.7}$$

where:
d_i is the difference between each pair of rank ($d_i = x_i - y_i$);
n is the volume of the sample.

The range of the value of ϱ is from -1 to 1. The negative means that with the increase of one variable the other is decreasing. It does not only depend on the relation between the variables, but also affected by the volume of sample. So there is necessary to do the significance testing.

3.6. Water sampling

3.6.1. Decide the sample locations

The sample locations were selected to reveal the spatial distribution of water quality parameters. It was assumed that spatial differences occurred after the old tube was closed and a new canal was opened on the edge of the wetland. So 11 measure points (Figure 3.3) were chose along the new canal and the old canal.

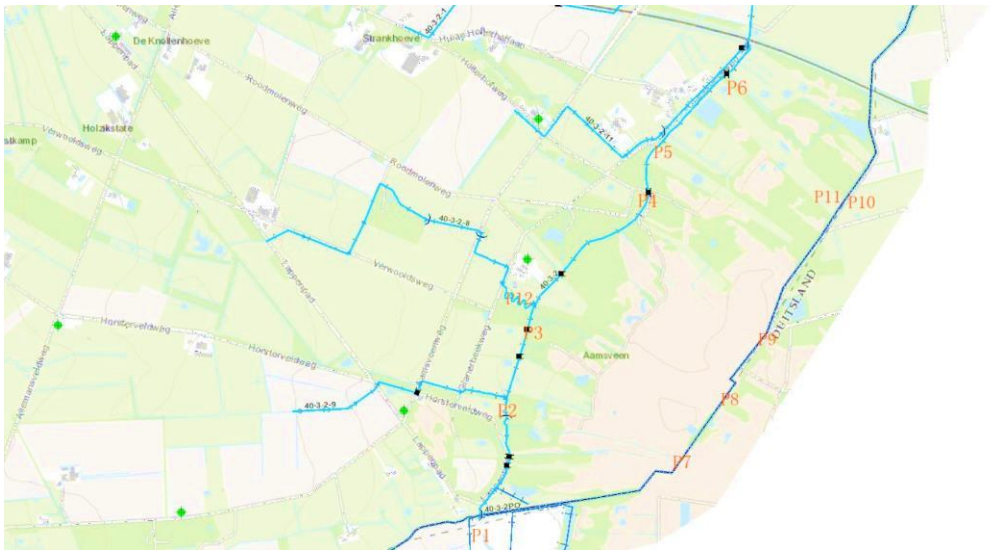

Figure 3.3: Water sampling points

3.6.2. Field evaluation of water quality parameters

The following parameters were defined from the collected samples:
pH, Conductivity, Temperature (in situ measurements)
Nitrate, Nitrite, Ammonia, Phosphate (laboratory analysis)

3.6.3. Water sampling

With Horiba U10, the pH, conductivity and temperature were measured on the spot. For every time, 3 samples (100 ml) were taken in one location. The water samples were filtered in the field, then acidified with 2 or 3 drops of hydrochloric acid to make the pH lower than 4 for the transport to the laboratory.
Nutrient parameters were analysed in the laboratory with a HACH spectrophotometer, which use a function of wavelength to measure the reflectance or transmittance of a material.
Here is the plan list to explain the sampling project (Table 3.2)

Table 3.2: Sampling details Table

Sampling Data	Sampling Amount	Parameters	
		Measured in filed	Measured in laboratory
23 Oct	9 (p1,p2,p3,p4,p5,p7,p8,p9, p12)	pH Conductivity Temperature	NO_3^-, $N0_2$-, and PO_4^{3-}
8 Nov	12 (p1,p2,p3,p4,p5,p6,p7,p8,p9,p10,p11,p12)	pH Conductivity Temperature	NH_4^+, NO_3^-, $N0_2$-, and PO_4^{3-}
22 Nov	11(p1,p2,p3,p4,p5,p6,p7,p8,p9,p10,p11)	pH Conductivity Temperature	NH_4^+, NO_3^-, $N0_2$-, and PO_4^{3-}

3.7. Accuracy assessment

3.7.1. RMSE for Interpolation Accuracy Assessment

For the Global Polynomial Interpolation, an accuracy assessment was carried out. Due to the low number of groundwater observation wells, bootstrapping (sampling with replacement) was used for leaving out one point each time and repeating the polynomial interpolation for each subsets. Root mean square error (RMSE, Figure 3.11) was calculated to compare the interpolated groundwater level with the measured groundwater level. This method was used for both the 1st and the 2nd order GIP results for 2013 and 2012.

$$RMSE = \sqrt{\frac{\sum_{i=1}^{n}(r_{Mi}-r_{gi})^2}{n}} \quad (3.8)$$

where:
r_M is the measured ground water level;
r_g is the retrieved groundwater level by global polynomial interpolation model;
n is the total band numbers.

3.7.2. Comparison with surface reflectance

After finishing the atmospheric correction, it's necessary to test its accuracy. Since there are no measured in situ reflectance values available from the acquisition dates, the verification was done relatively, between the two resulting images. The following steps were made:

1. Checking the Google Earth to find two different but smooth and non-changing surfaces. One bright with high reflectance (this was a bright roof), and the other one dark (a dark roof) that can maximally absorb solar radiation;
2. Extracting the surface reflectance of the two points in 2004, and 2014;
3. Comparing these data by constructing the regression line.

4. RESULTS AND DISCUSSION

4.1. Vegetation change map

4.1.1. Vegetation detection

The maps of vegetation structure in both years were combined into a change map using the Intersect function in ArcGIS. The areas with the same vegetation structure type were considered as unchanged areas (Figure 4.1). The areas with different vegetation structures were further studied based on the original vegetation description. They represented actual vegetation changes, but also slight or almost no differences in comparison to the original vegetation type description. This latter is due to differences in details of mapping, both in scale and thematic detail.

The real changes can be explained as natural changes from meadow or agriculture to areas with no agriculture practice (so called 'new nature'). The different types of change are:
-1. Meadow changed to grassland with Juncus;
-2. Agriculture changed to nettle;
The distribution of these areas can be seen in Figure 4.2.b
Very tiny polygons were disregarded in the final output, as these are caused by the methodology (Westinga et al, 2013), and are not real changes.

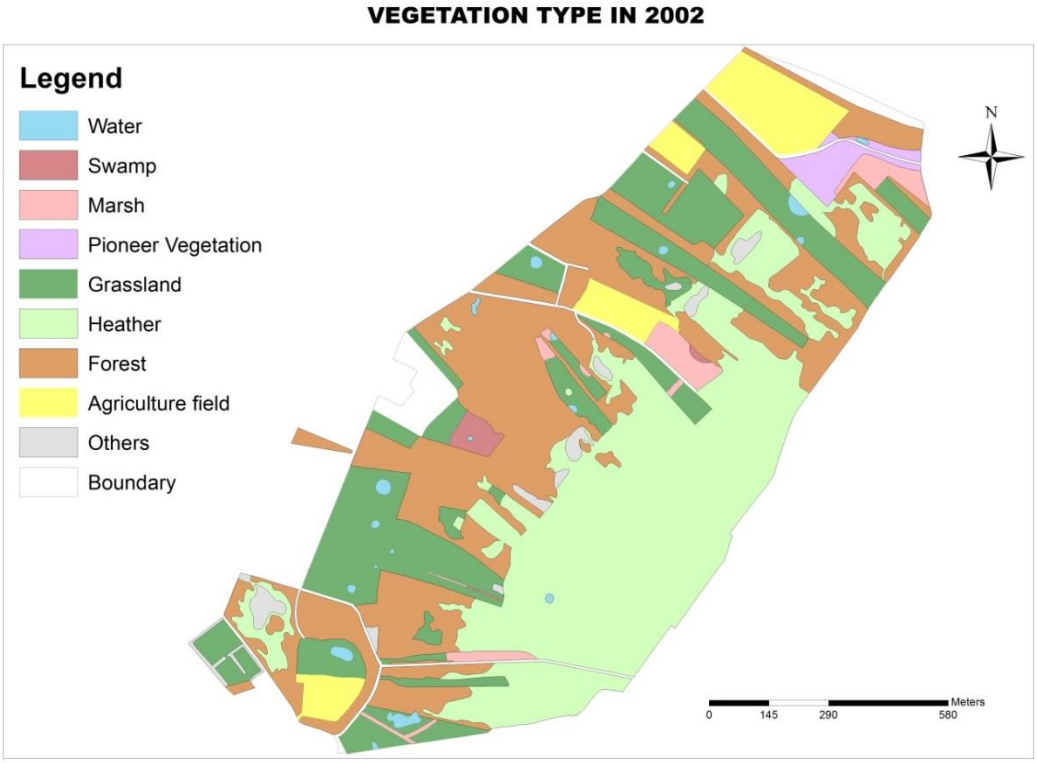

(a)

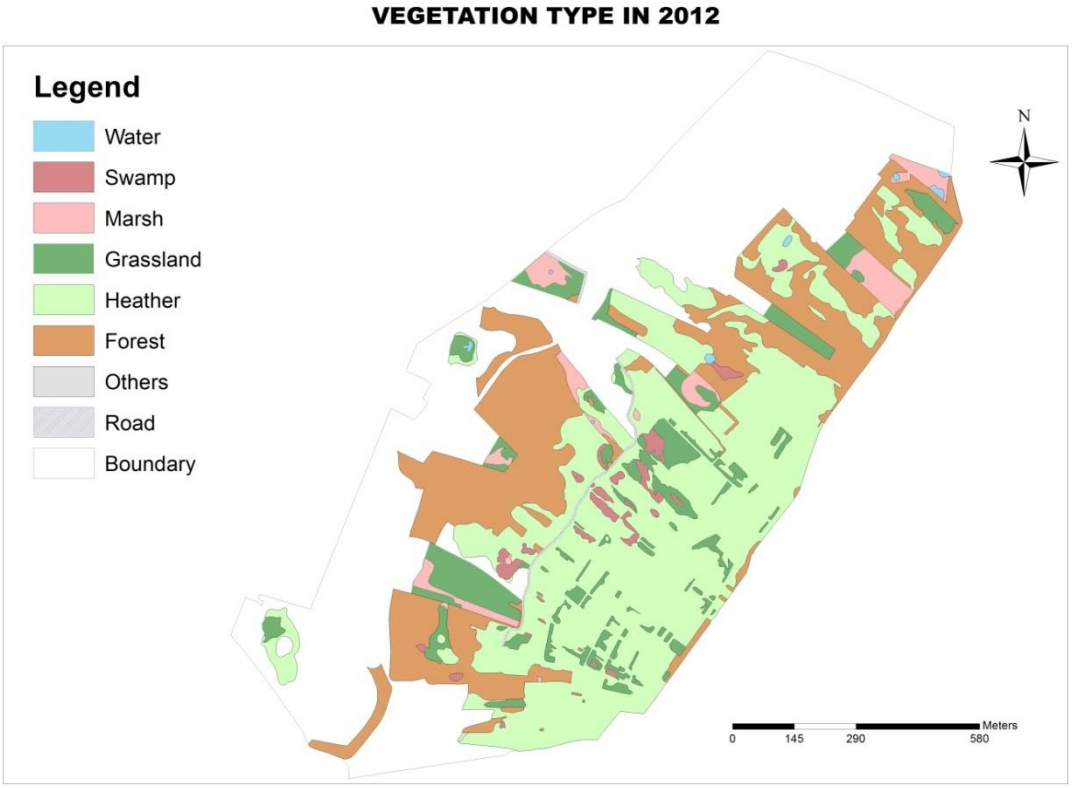

(b)

Figure 4.1: Vegetation maps. (a) Vegetation type in 2002 (b) Vegetation type in 2012

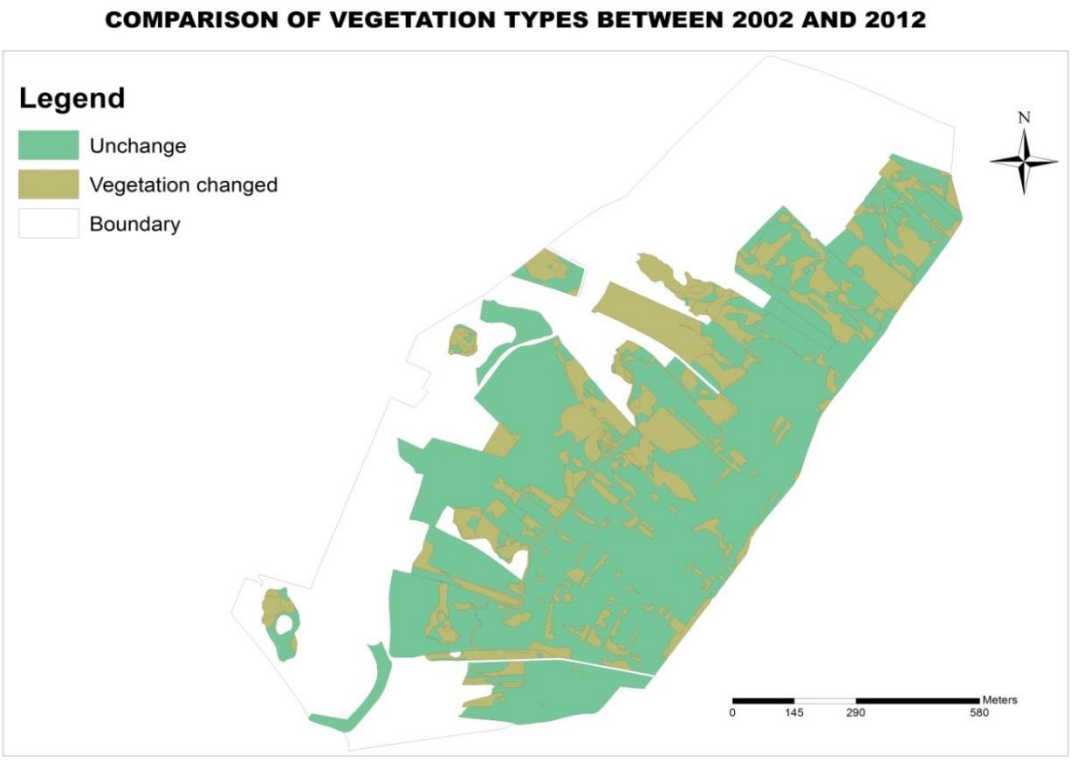

(a)

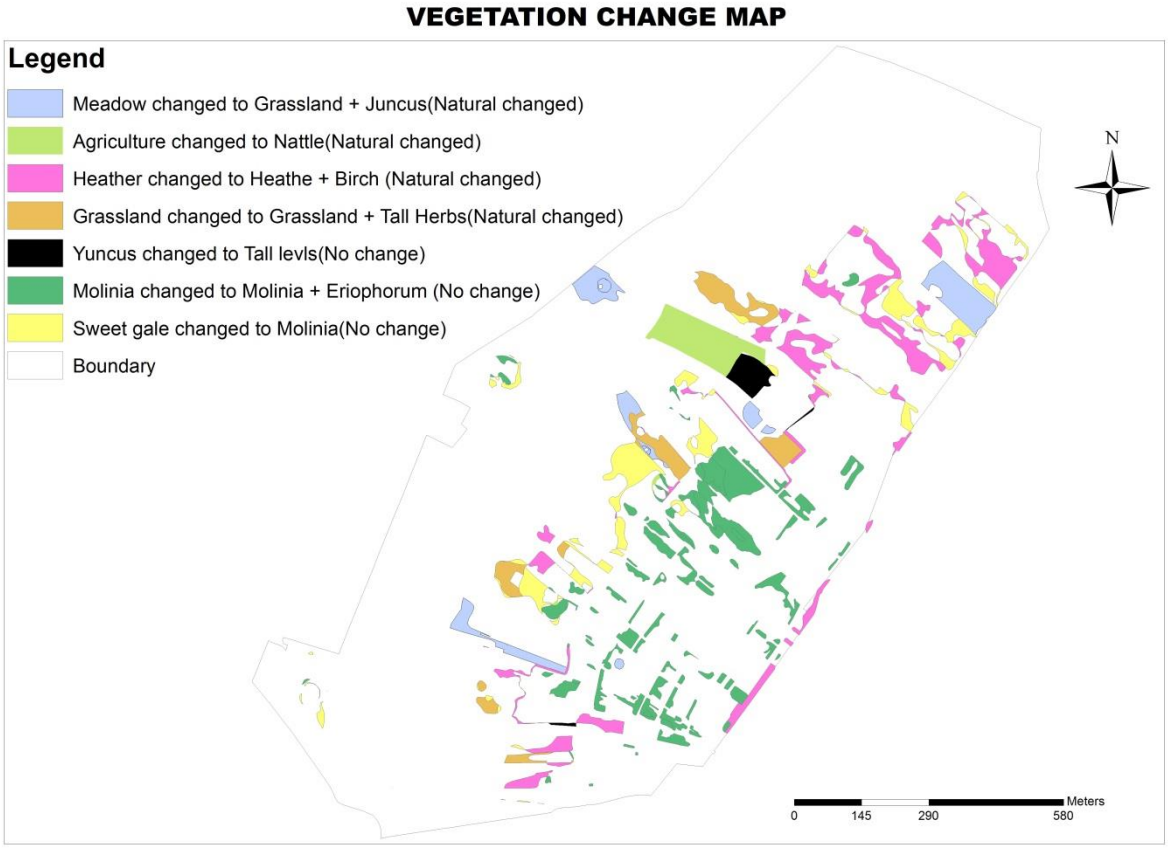

(b)

Figure 4.2: Change detection. (a) Variation of vegetation (b) Details of the changed

Figure 4.2a shows the changed and unchanged areas of vegetation generally. The large green area is the dominant species have not changed in 10 years. It occupies most of the wetland. The changed areas are few and speared around the whole area. Its map, Figure 4.2b was used for the analysis of the changed area to see if the change is true.

The blue shows the meadow changed to grassland with Juncus; the light green presents the agriculture changed to nettle. Both these changes can be expected after stopping agricultural practises management. The pink displays the heather changed to heater with birch, i.e. some birch trees encroach into this area; the orange shows grassland changed to grassland and tall herbs. These changes are natural successions.

The black area shows the *Juncus* changed to the tall herbs; these two classes are almost the same. The dark green area means the *Molinia* changed to *Molinia* with *Eriophorum*; and the yellow area present the sweet gale changed to *Molinia*. The differences is small, most probably caused by different levels of detail of the mapping

4.1.2. NDVI

4.1.2.1. Atmosphere correction

After atmospheric correction, the images have more contrast (Figure 4.3). The validation of the atmosphere correction was done to test the results (Figure 4.4). The X-axis is the reflectance of white and black roofs in 2004 and the Y-axis is the reflectance of white and black roofs in 2014. From the results, we can see the reflectance in different year fit very well both on the black roof and the white roof, proving that the results of atmosphere correction are credible.

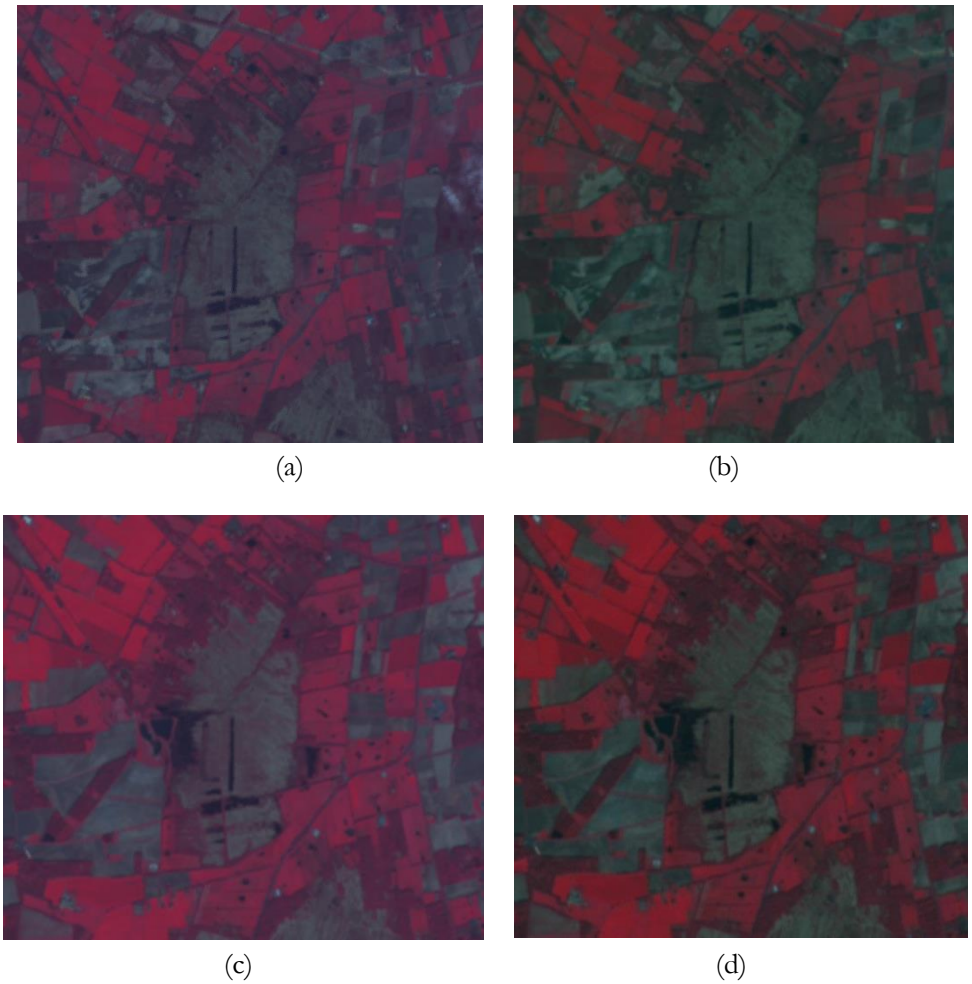

(a) (b)

(c) (d)

Figure 4.3: Atmospheric correction results.(a) Before atmospheric correction (2004. April) (b) After atmospheric correction (2004 April) (c) Before atmospheric correction (2014 April) (d) After atmosphere correction (2014 April)

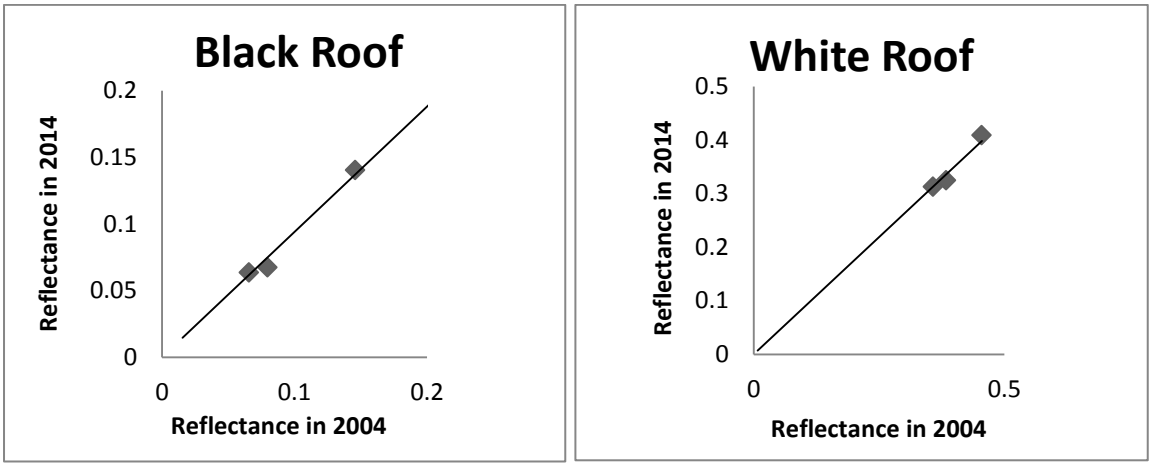

(a) (b)

Figure 4.4: Comparison of atmospheric correction results between 2004 and 2014

4.1.2.2. NDVI

After atmospheric correction, the NDVI for the two years were calculated by the Equation 3.4. The comparison of NDVI was calculated by the Equation 3.5. The value of dark area is lower than the value of white area. From the Figure 4.5.a, it shows that most area in Aamsveen is in dark colour in 2004. But the colour in Aamsveen in 2014 is brighter (Figure 4.5.b). It means the vegetation grows well in the 10 years in general. In the Figure 4.5.c, the colour of images looks uniform in the wetland area.

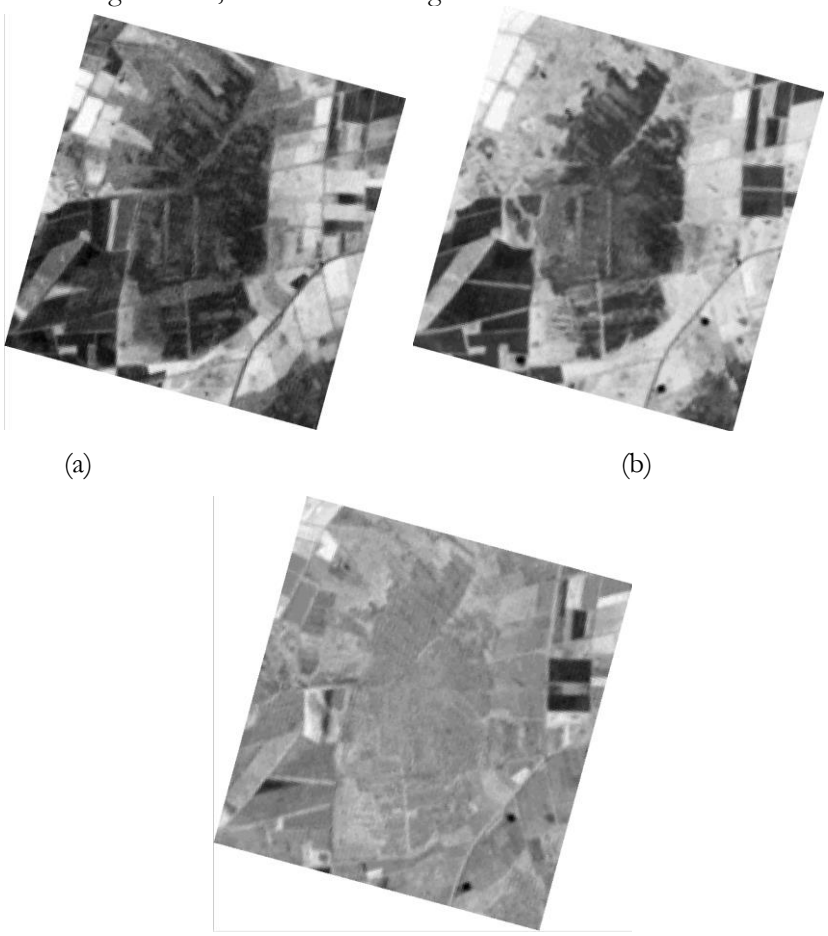

(a) (b)

(c)

Figure 4.5: NDVI maps (a) NDVI map in 2004; (b) NDVI map in 2014; (c) NDVI difference map between 2004 and 2014

To get more information about the vegetation, the histograms of the previous three NDVI maps were extracted out (Figure of 4.6, 4.7, and 4.8). The Figure 4.6 presents that the peak of the NDVI is around 0.3, and all the values are above 0. In the Figure 4.7, the first pick is also around 0.3, but there is a second peak of this around 0.7, which means a greener wetland, i.e. the vegetation was more developed in 2014. And most of the value of NDVI difference between 2004 and 2014 is above 0. It means the vegetation keeps growing in most area of the images.

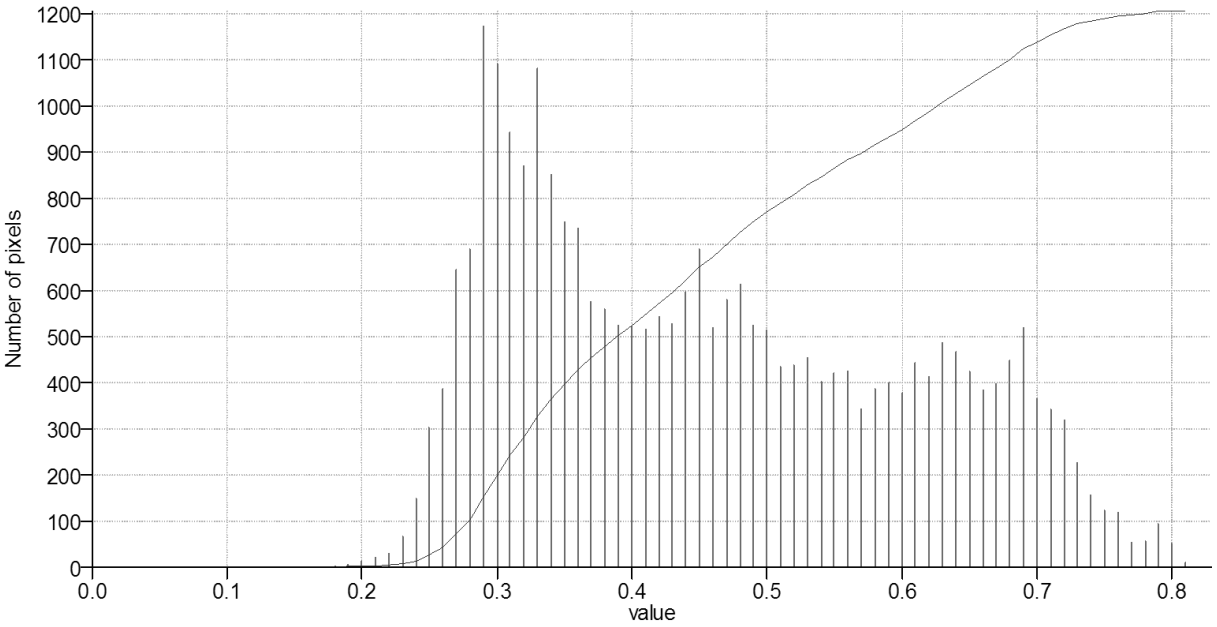

Figure 4.6: Histogram of NDVI for 2004

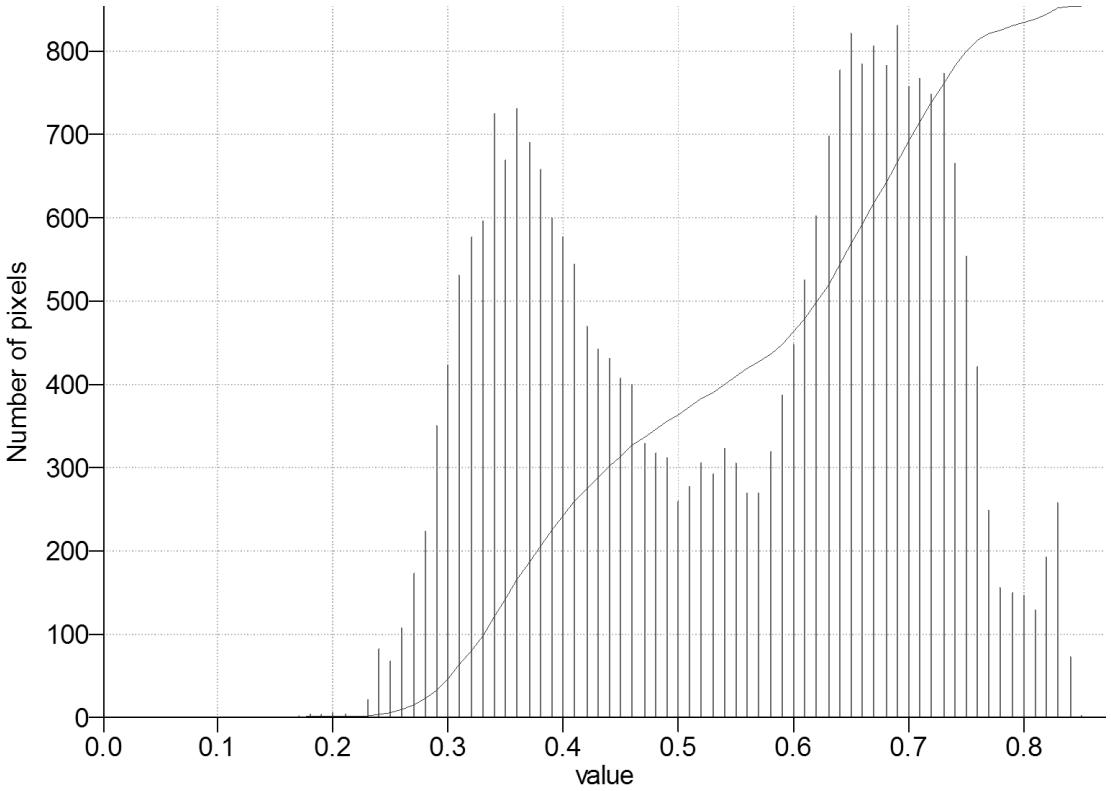

Figure 4.7: Histogram of NDVI for 2014

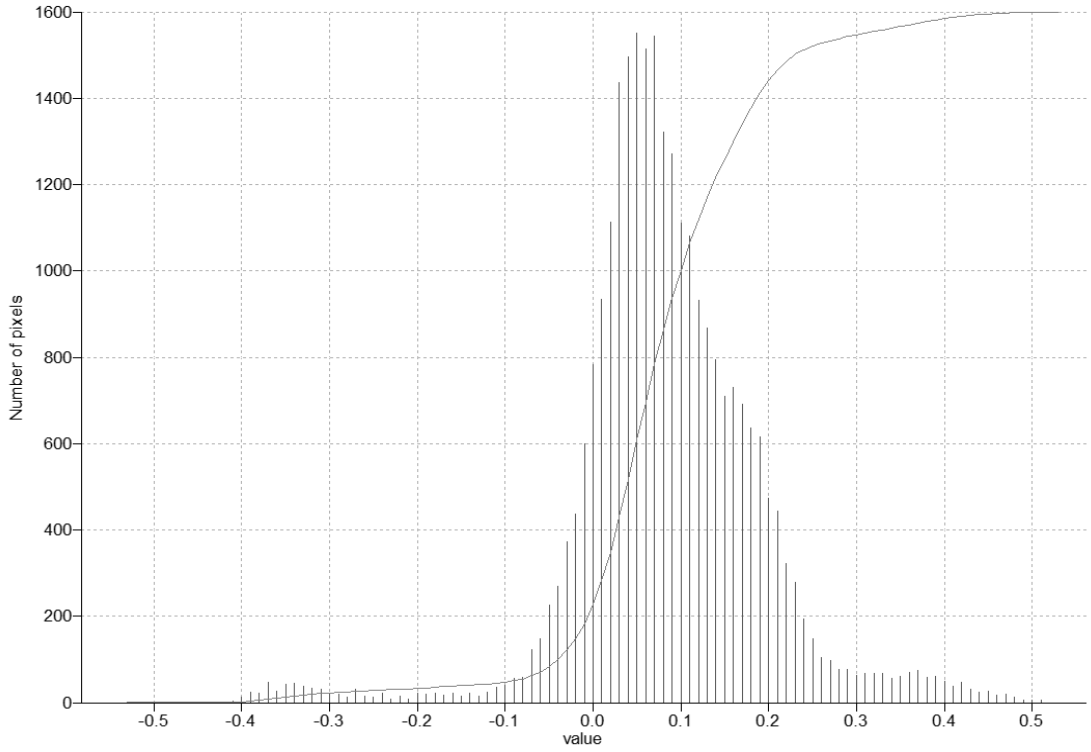

Figure 4.8: Comparison of NDVI in 2004 and 2014

4.2. Results of statistical analysis for hydrology part

There are 11 monitoring points for groundwater (Figure.4.9), they are distributed in the Aamsveen in a random-looking pattern. B35A0194 is located at the upstream part of the wetland, where the canal enters it, and B35A0196 is located near the outflow. Figure 4.10 shows the overview of the monthly groundwater depths. It shows that the groundwater level in the point of B35A0194 always the highest, and the B35A0197 and B35A0196 are the lowest almost all the time. The reason is that both the old canal and the new canal come from the point B35A0194 and flow out at point B35A0196. The major direction of the groundwater flow most probably coincides with the surface flow. But only from individual point observations it is hard to tell the change of wetland's groundwater system, so trend and correlation analysis were used to analyse it.

Figure 4.9: Groundwater measure points in Aamsveen

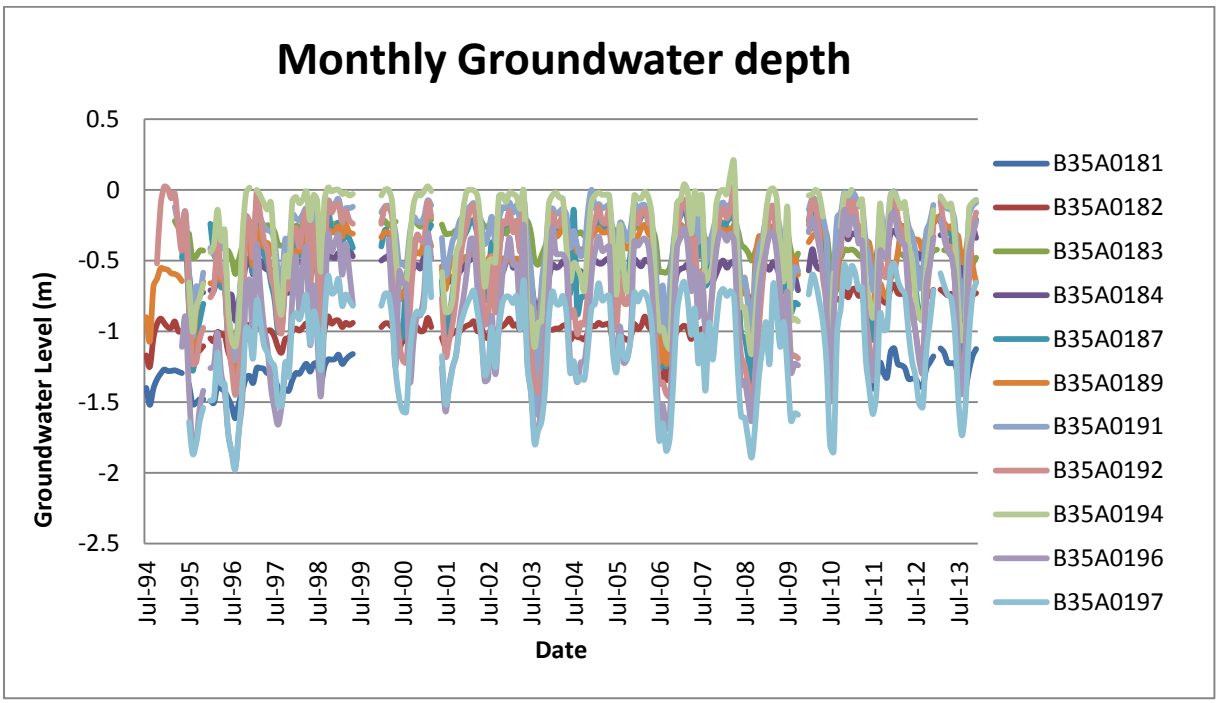

Figure 4.10: Monthly groundwater depth

Before all the analysis, it's important to define the wet season and dry season for the recent 19 years in the region of the wetland. The difference of precipitation and evaporation is negative from April to August (Figure 4.11). This means, that the wetland loses water in this period. The groundwater level measurements prove this. Take the groundwater level in 192 as an example (Fig.4.12), due to the location of it is in the middle area of the wetland. From the Fig 4.12 , the groundwater level is lower in the summer. The difference between precipitation and evaporation is positive from September to next year's March, and the groundwater level is higher. So the dry season is from May to August, and the wet season is from November to next year's February.

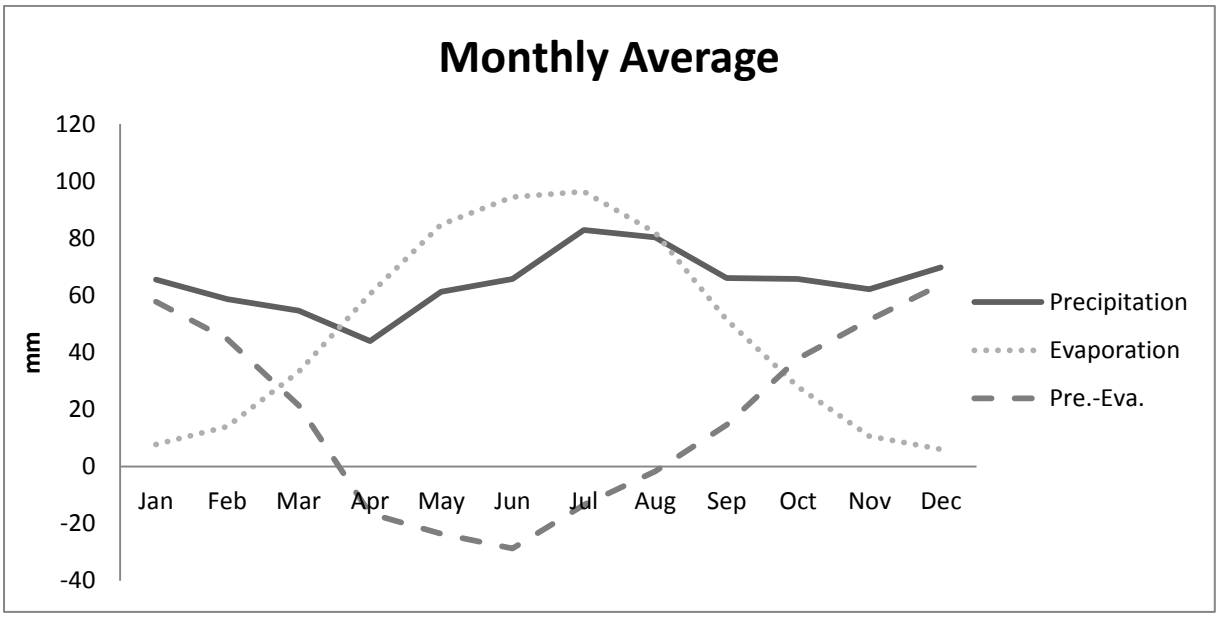

Figure 4.11: Monthly average values of precipitation, evaporation, and precipitation-evaporation for the period of 1995-2014

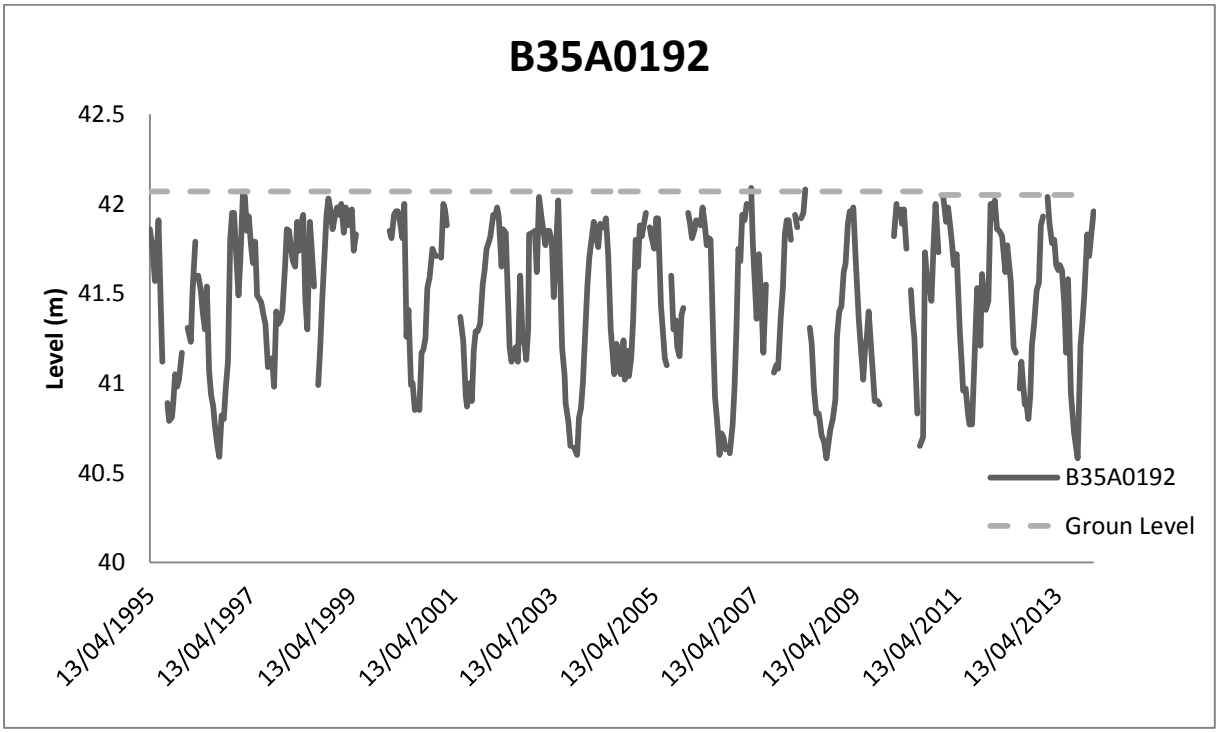

Figure 4.12: Groundwater level and groun level in the point of B35A0192

4.2.1. Absolute RMSE for GIP

Since the limitation of the data and the interpolation methods, it would lead the absolute RMSE not small. In order to test the accuracy of the method, we take the data of 2013 as example to compare. The results are shown in Table 4.1.

Table 4.1: Absolute RMSE for GIP in 2013 and 2012

	RMSE
1st order GIP for dry season in 2013	0.506328
1st order GIP for wet season in 2013	0.548838
2nd order GIP for dry season in 2013	0.47567
2nd order GIP for wet season in 2013	0.24438
1st order GIP for dry season in 2012	0.4692194
1st order GIP for wet season in 2012	0.496519
2nd order GIP for dry season in 2012	0.4574648
2nd order GIP for wet season in 2012	0.394531

From the Table 4.1, we can see that the 2nd order Global Polynomial Interpolation is better than 1st order GIP. And absolute RMSE of the GIP for the dry season are lower than wet season. However, the results still showed a desired fit between retrieved groundwater level and original groundwater level.

4.2.2. Results of Global Polynomial Interpolation

There are only two year's data (2012, 2013) available after the canal change. As the year of 2012 is only one year later after the canal changed, so the data of 2013 was used to do the comparison. The annual precipitation in 2013 was 751.6 mm, the annual potential evaporation in 2013 was 558.7 mm, and the difference between annual precipitation and potential evaporation is192.9 mm. These are close to the average values of this region. The data of 2005 are close to the data in 2013. The annual precipitation in 2005 was 797 mm, the annual potential evaporation in 2005 was 590.7 mm, and the difference between annual precipitation and potential evaporation is 206.3 mm (Appendix C).

From the patterns of the trends (Figures 4.13 and 4.14), no major change can be seen neither with the 1st nor with the 2nd order polynomials.

The differences are smaller than the RMSE (Table 4.1) of the interpolation maps. Therefore, no significant conclusion can be drawn. Still, some spatial probable conclusions can be made about the spatial patterns of the differences.
The difference maps with the 1st order polynomial interpolation show that in the dry season, the groundwater became lower at the new canal, whilst it hardly changed at the old canal. And in the wet season, the difference is around zero. The difference maps (Figure 4.15) with the 2nd order polynomial interpolation suggest that the changes may be larger close to the canals.
Nevertheless, no significant changes happened so far in average years, but it cannot be concluded how the water regime would react on extremely dry or extremely wet conditions.

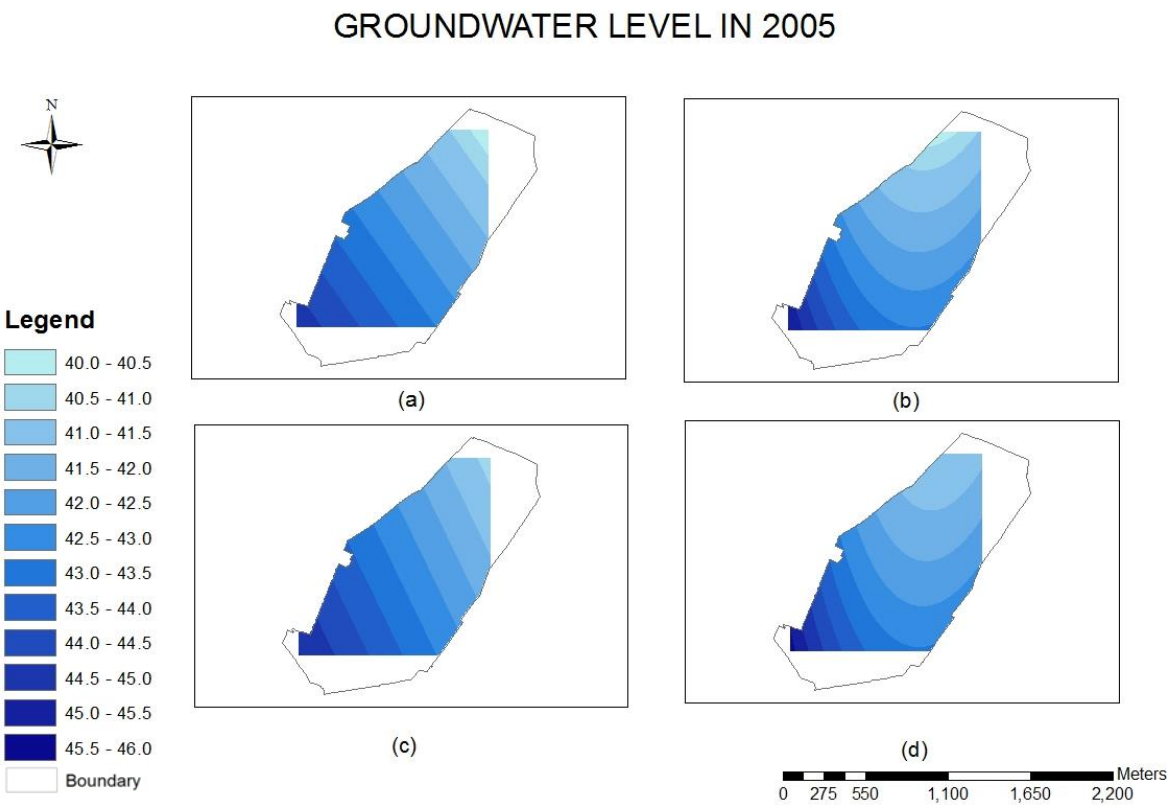

Figure 4.13: Global Polynomial Interpolation results for 2005. (a) 1st order GIP for dry season (b) 2st order GIP for dry season (c) 1st order GIP for wet season (d) 2st order GIP for wet season

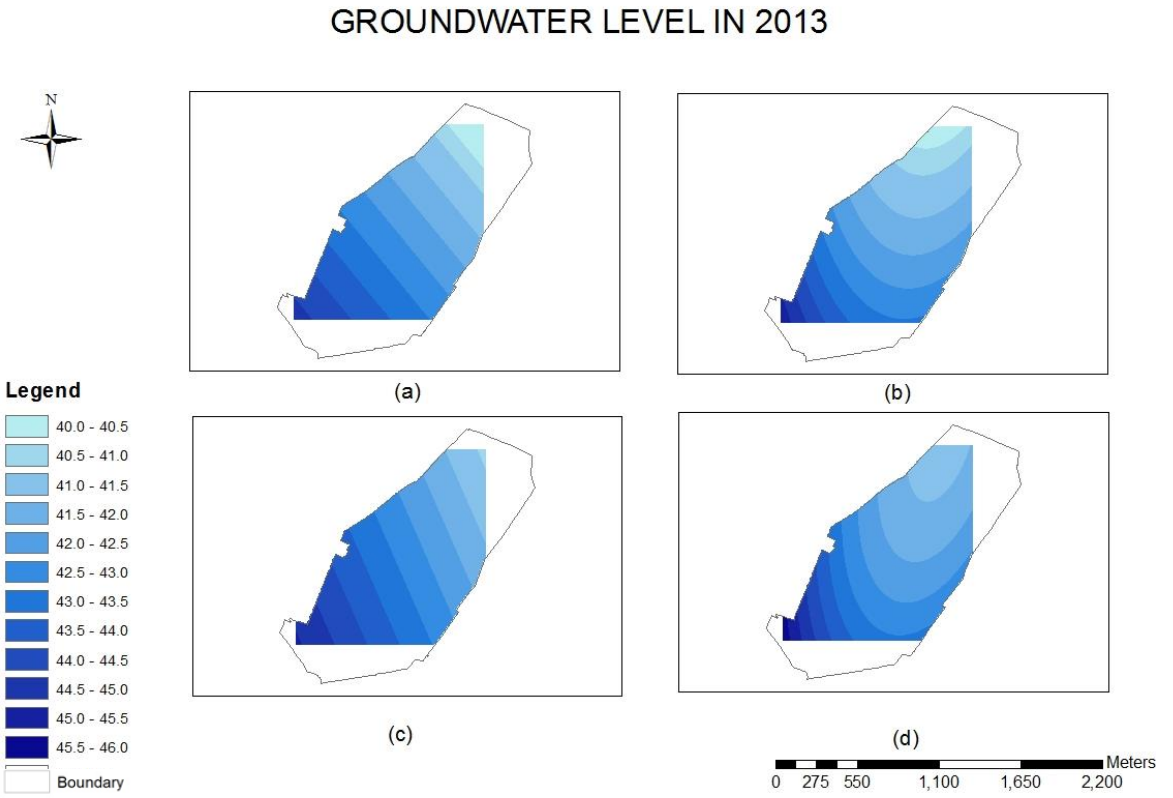

Figure 4.14: Global Polynomial Interpolation results for 2013 (a) 1st order GIP for dry season (b) 2st order GIP for dry season (c)1st order GIP for wet season (d)2st order GIP for wet season

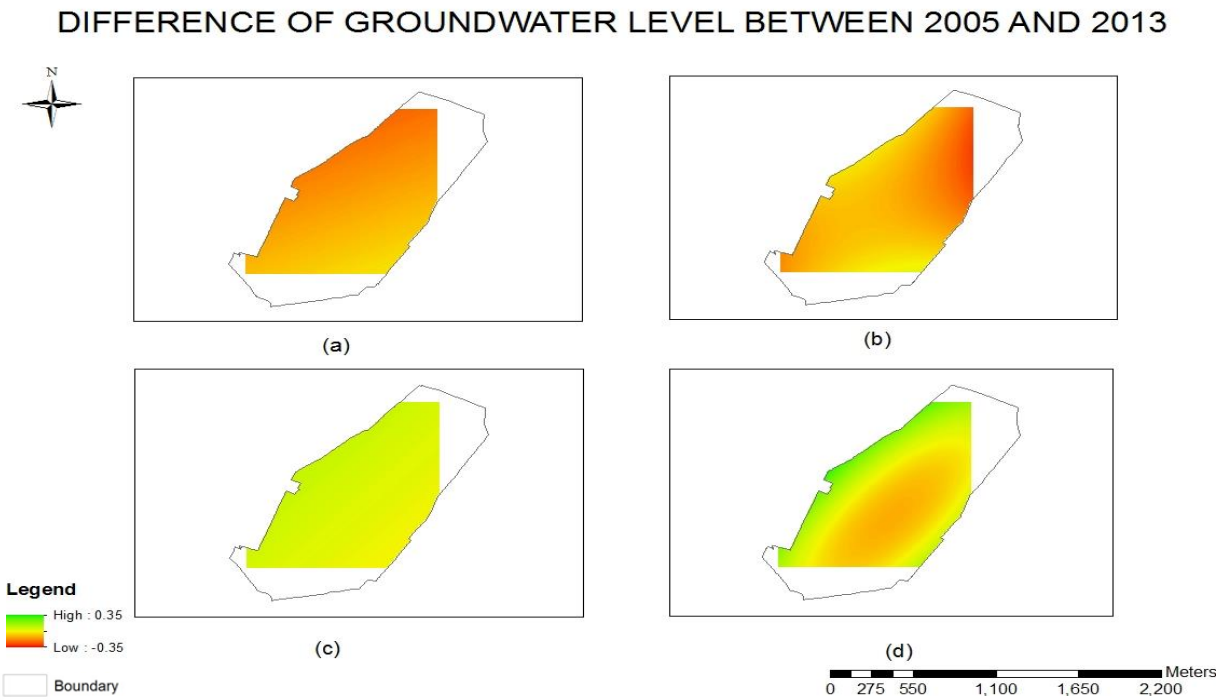

Figure 4.15: Comparison of groundwater levels between 2005 and 2013 (Difference=2013-2005) (a) Difference for dry season with 1st order GIP (b) Difference for dry season with 2st order GIP (c) Difference for wet season with 1st order GIP (d) Difference for wet season with 2st order GIP.

The driest year and wettest year were defined for the period of 1995-2014. It was found that 2007 was the wettest year and 2003 was the driest year: the annual precipitation in 2007 was 915.5 mm; the annual potential evaporation in 2007 was 565.5 mm, so the difference between annual precipitation and potential evaporation is 350 mm. The annual precipitation in 2003 was 616.6 mm; the annual potential evaporation in 2003 was 642.4mm, so the difference between annual precipitation and potential evaporation is -25.8mm. `

From the patterns of the trends (see Figures 4.16 and 4.17), no major change can be seen neither with the 1st nor with the 2nd order polynomials as well. But combine the Figures 4.13 and 4.14, the tendency of the groundwater level won't change no matter in wet season or dry season.

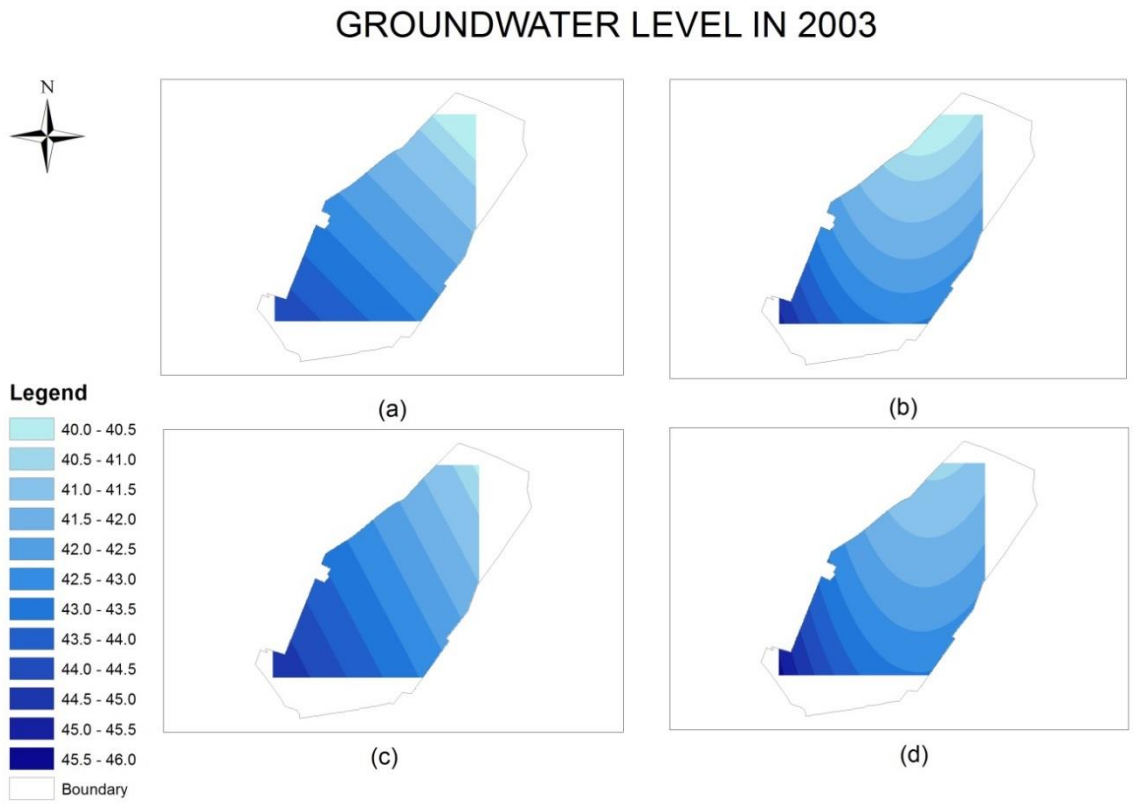

Figure 4.16: Global Polynomial Interpolation results for 2008. (a) 1st order GIP for dry season (b) 2st order GIP for dry season (c) 1st order GIP for wet season (d)2st order GIP for wet season

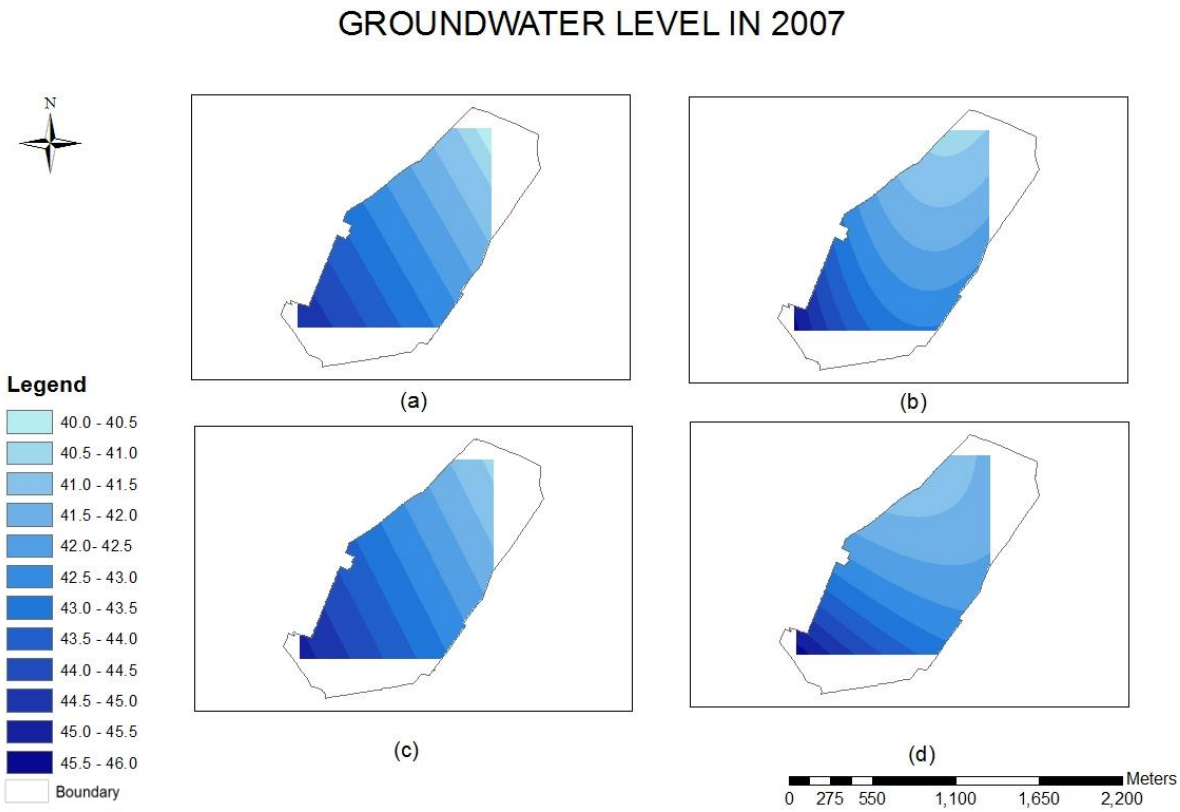

Figure 4.17: Global Polynomial Interpolation results for 2007. (a) 1st order GIP for dry season (b) 2nd order GIP for dry season (c) 1st order GIP for wet season (d)2nd order GIP for wet season

4.2.3. Results of correlation analysis

Due to the uncertainties of the groundwater interpolation, the relation between groundwater and the other hydrological parameters has to be analysed using the individual well observations.

Table 4.2 shows the correlation coefficients between groundwater level, precipitation-evaporation and flow for the period before and after the canal redirection. The value of correlation coefficient is larger; the relationship between them is more outstanding. Precipitation can't affect groundwater alone after canal changed. But evaporation, water budget of precipitation and evaporation, and flow make greater effects on groundwater level. And flow still affects groundwater level greatly. After the canal change, the influence of the Precipitation-Evaporation was increasing, which means these wells are more working on precipitation and evaporation now, and that was effected by the old canal. Due to the correlation coefficient increase, that means these wells are under the influence of the new canal.

Table 4.2: Correlation coefficient between groundwater level, precipitation-evaporation and flow (before and after Sep. 2011)

	Precipitation-Evaporation		Flow	
	Before	After	Before	After
Groundwater Level_181	0.309**	0.538**		
Groundwater Level_182	0.476**	0.570**	0.578**	0.822**
Groundwater Level_183	0.196**	0.356*	0.386**	0.782**
Groundwater Level_184	0.305**	0.519**	0.446**	0.791**
Groundwater Level_187	0.483**	0.609**	0.609**	0.897**
Groundwater Level_189	0.410**	0.666**	0.292**	0.878**
Groundwater Level_191	0.492**	0.551**	0.574**	0.84**
Groundwater Level_192	0.460**	0.525**	0.591**	0.836**
Groundwater Level_194	0.456**	0.549**	0.524**	0.821**
Groundwater Level_196	0.462**	0.581**	0.650**	0.893**
Groundwater Level_197	0.478**	0.478**	0.819**	0.816

One asterisk means there is a significant correlation between two variables when α is 0.05; two asterisks means there is a significant correlation between two variables when α is 0.01. If there is no asterisk after correlation coefficient, then there is no significant correlation between two variables.

4.3. Results of Water quality

According to the United States Environmental Protection Agency (EPA) water quality criteria state that phosphates should not exceed 0.1 mg L^{-1} in streams or flowing waters discharging into lakes or reservoirs to control algal growth ("Water Resource Characterization DSS - Phosphorus,"). But the final results are extremely high, which are not reliable. The other values all look reliable, proving that the instrument has little responsibility in the errors. So, the mistakes may be caused by the dilution during the laboratory analysis. Due to all the samples were diluted with the same method, the relative differences between the different samples are credible. Therefore, the concentrations of phosphates were replaced by the relative level of concentrations. The classification is very high (VH), high (H), medium (M), low (L), very low (VL).

Table 4.3 : Sampling in 23 Oct (9 points)

	Distance(m)	pH	Cond.(mS/cm)	T(°C)	NO3-N	N02-N	PO43-
1	0	7.7	0.425	11.8	1.3	0.002	VH
2	300	6.86	0.476	12.7	14.5	0.012	M
3	540	6.06	0.376	12.1	4.4	0.004	L
4	915	5.64	0.344	11.5	3	0.017	M
5	1020	5.45	0.345	11.3	2.7	0.004	M
12	540	6.06	0.376	12.1	4.4	0.004	L
	Distance(m)	pH	Cond.(mS/cm)	T(°C)	NO3-N	N02--N	PO43-
7	540	4.55	0.083	10.9	14.5	0	L
8	735	4.27	0.083	10.8	14.7	0.004	L
9	915	3.74	0.104	12	16.8	0	L

Table 4.4: Sampling in 8 Nov (12 points)

	Distance(m)	pH	Cond.(mS/cm)	T(°C)	NH4+	NO3--N	N02--N	PO43-
P1	0	6.97	0.449	10.2	1	3.2	0.068	H
P2	300	7.13	0.458	10	0.5	4.4	0.112	M
P3	540	6.44	0.437	9.2	0.2	4.6	0.009	M
P4	915	6.37	0.384	9.8	0.2	3.9	0	M
P5	1020	5.55	0.382	9.2	0.3	3.9	0	H
P6	1260	6.12	0.383	9.8	0.2	3.9	0	L
P12	540	6.58	0.396	9.8	0.1	8.7	0.003	H
	Distance(m)	pH	Cond.(mS/cm)	T(°C)	NH4+	NO3--N	N02--N	PO43-
P7	540	4.24	0.084	9.4	2	6	0	VH
P8	735	4.04	0.087	8.7	3	6	0	M
P9	915	3.49	0.1	10.2	0.6	6	0	L
P10	1312.5	5	0.11	10.4	0.5	5	0	L
P11	1312.5	4.13	0.076	10.2	0.1	6	0	L

Table 4.5 : Sampling in 22Nov (11points)

	Distance(m)	pH	Cond.(mS/cm)	T(°C)	NH4+	NO3--N	N02--N	PO43-
p1	0	7.2	0.675	9.3	1	4.65	0.0025	H
p2	300	6.89	0.749	8.3	0.6	6.35	0.0075	H
p3	540	6.34	0.712	7.1	0.3	7.15	0.003	H
p4	915	6.09	0.631	7.1	0.1	5.6	0	H

p5	1020	5.5	0.733	7.4	0.05	5.35	0	H
p6	1260	6.14	0.8	7.3	0	3.95	0.002	M
p11	540	6.34	0.716	8.4	0.4	11.6	0.0015	L
	Distance(m)	pH	Cond.(mS/cm)	T(°C)	NH4+	NO3--N	N02--N	PO43-
p7	540	4.49	0.162	7.5	3	4	0	VH
p8	735	4.25	0.365	8.1	4	3.65	0	VH
p9	915	3.45	0.156	8.6	2	4.45	0.009	H
p10	1312.5	3.57	0.192	8.1	0.05	3	0.014	M

The changes of the nutrient concentrations along the new and the old canal are shown in Figure 4.14. The acronyms for legends are the following:
1(n): 23-Oct in new canal
2(n): 08-Nov in new canal
3(n): 22-Nov in new canal
1(o): 23-Oct in old canal place
2(o): 08-Nov in old canal place
3(o): 08-Nov in old canal place

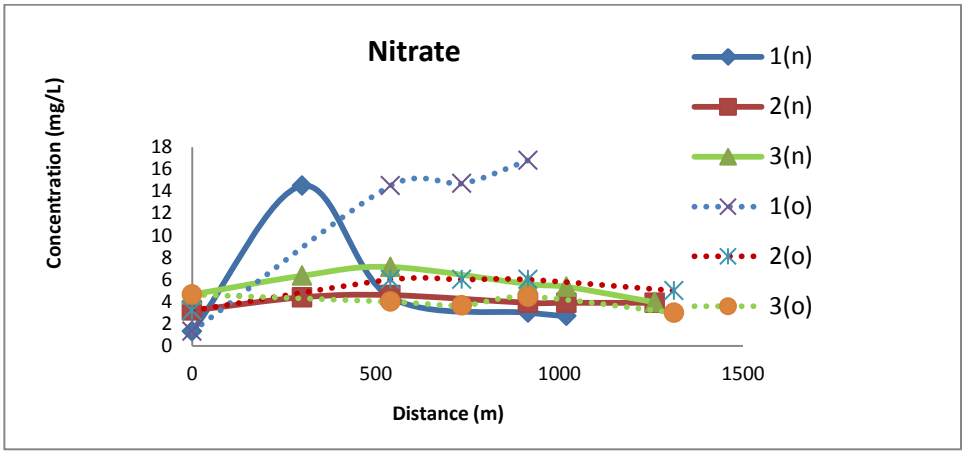

(a)

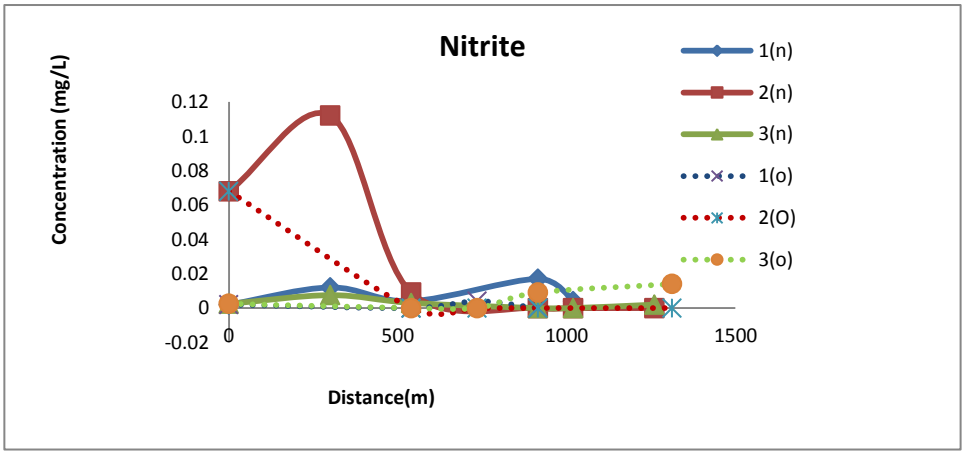

(b)

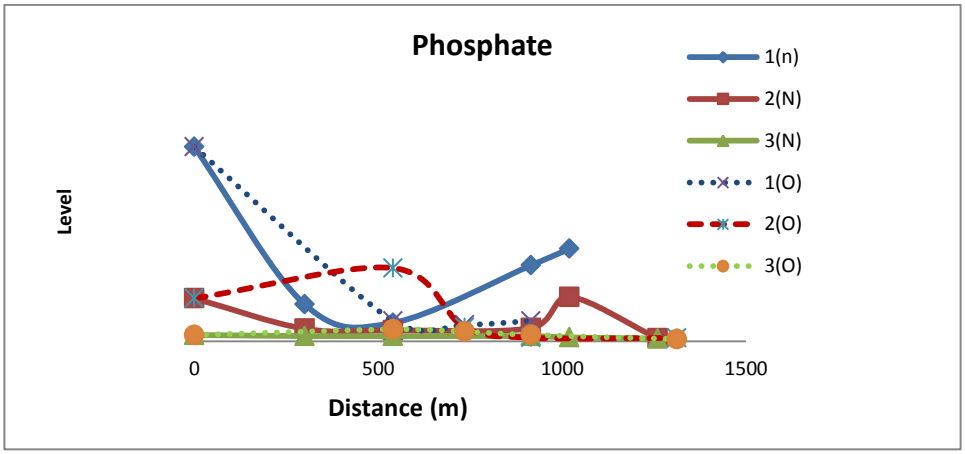

(c)

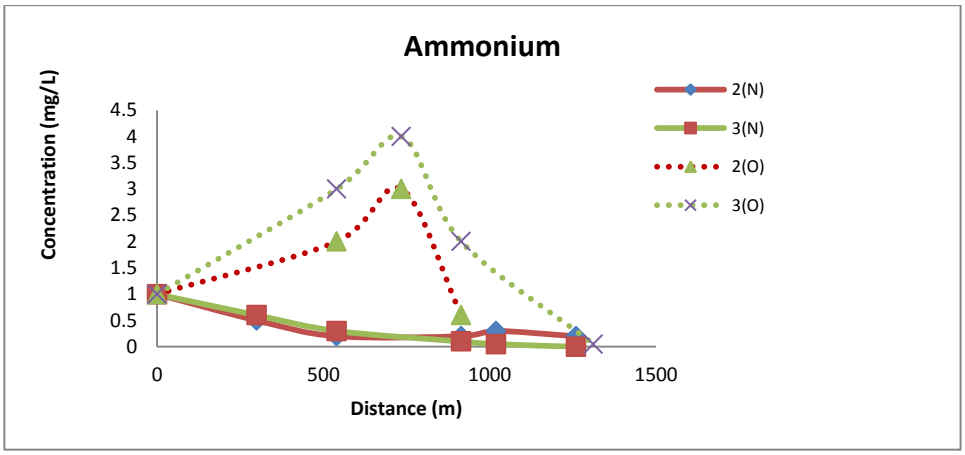

(d)

Figure 4.18: Comparison of Nutrite concentration between the new canal and the old canal in 3 different times.(a) Nitrate(b) Nitrite (c) Phosphate (d) Ammonium

The sampling points are shown in the Figure 3.3. The highest values for nutrient parameters in the new canal are around point 3. Since there is a canal flowing into the new canal at point 3, it is proved that the catchment of the tributary canal loads the wetland with the nutrients. The nitrate, nitrite and phosphate are also kept same in the old canal.

For the nitrate and nitrite concentration, the values of new canal are higher than old canal. But the values of phosphate and ammonium are lower in the new canal. But in general, the canal would mean external load on the wetland, so it is good that it had been diverted from the old route, which was going in the middle of the wetland. The old canal does not show this load, so it is well separated from the external influence.

5. CONCLUSION AND RECOMMENDATIONS

5.1. Conclusion

The main objective was to analyse the effect of altering the course of the draining canal in the Aamsveen on the vegetation and water cover by combining field and remote sensing techniques. There were five main aspects of achieving the objective: vegetation detection, NDVI analysis, Global Polynomial interpolation of groundwater levels, statistical analysis of hydrological data, and the analysis of the distribution of the nutrients in the canals based on field data. Vegetation map analysis provided the details of the vegetation changes since 2002. NDVI showed the growth situation of vegetation generally. Global polynomial interpolation explained the groundwater level trends in the wetland. Statistical methods revealed the relationship between the groundwater level, precipitation-evaporation and flow. The filed work illustrated the nutrients' spatial distribution in the new canal and the old canal.

The following conclusions can be drawn from the present results:

1. Vegetation change analysis: some of the vegetation changed because of the natural succession. The other change is minor, and could not be related significantly to groundwater changes. Therefore, none of these changes were proved to be caused by the groundwater change or water quality change. Overall, the canal change hasn't affected the vegetation distribution significantly since 2011. But the results of NDVI show that the vegetation grows well, and the vegetation in the Aamsveen is thicker than in 2004.

2. Groundwater level analysis: the difference of groundwater between the canal change before and after is smaller than the mapping accuracy. Although the changes of the groundwater level, precipitation-evaporation and flow are relatively small since the redirection of the canal, the relationships between the groundwater level, precipitation-evaporation and flow have somewhat changed. The effect of precipitation-evaporation on some wells became more remarkable than before. The most correlated hydrological elements are the groundwater level and channel flow.

3. Water quality analysis: the new canal reduces a large part of the external nutritent load on the wetland. The concentrations of nitrite, phosphate and ammonium are higher in the canal flowing into the research area because of the agricultural lands. The concentrations of them are lower in the outflow from the wetland.

4. Since the results don't show any apparent relation between groundwater level and vegetation changes, the comparison of groundwater level, vegetation, and nutrient distribution can't be realized.

5. Since natural reaction of the vegetation on smaller changes in the water regime takes several years, a longer period is needed after the diversion of the canal for identifying the actual effects.

5.2. Recommendations

The results proved that the changes are of smaller magnitude what could be identified without doubts with the applied methods, so improvement based on this study is still needed in the further study. There are some recommendations:

1. More groundwater observation wells should be installed in the Aamsveen to observe the groundwater level within and around the boundary of Aamsveen.

2. The assessments of Aamsveen could be done in the future.

3. Two regular WQ observation points just at the inflow and the outflow points of the Aamsveen, plus one inside somewhere around the old canal.

LIST OF REFERENCES

Aerosol Robotic Network (AERONET) Homepage. (n.d.). Retrieved February 04, 2015, from http://aeronet.gsfc.nasa.gov/

Bajjali, W. (2012). Model the effect of four artificial recharge dams on the quality of groundwater using geostatistical methods in GIS environment, Oman. *Journal of Spatial Hydrology*, *5*(2). Retrieved from http://spatialhydrology.net/index.php/JOSH/article/view/39

Barnett, T. P., & Preisendorfer, R. (1987). Origins and Levels of Monthly and Seasonal Forecast Skill for United States Surface Air Temperatures Determined by Canonical Correlation Analysis. *Monthly Weather Review*, *115*(9), 1825–1850. doi:10.1175/1520-0493(1987)115<1825:OALOMA>2.0.CO;2

Bolboaca, S., & Jäntschi, L. (2006). Pearson versus Spearman, Kendall's tau correlation analysis on structure-activity relationships of biologic active compounds. *Leonardo Journal of Sciences*, (9), 179–200. Retrieved from http://ljs.academicdirect.org/A09/179_200.htm

Dams, J., Dujardin, J., Reggers, R., Bashir, I., Canters, F., & Batelaan, O. (2013). Mapping impervious surface change from remote sensing for hydrological modeling. *Journal of Hydrology*, *485*, 84–95. doi:10.1016/j.jhydrol.2012.09.045

Fassio, A. (2000). *peat bog regeneration.pdf*. University of Twente.

Field, A., Miles, J., & Field, Z. (2012). *Discovering Statistics Using R*. *Statistics* (Vol. 58, pp. 53–57). Retrieved from http://sro.sussex.ac.uk/38823/

Finn, M. P., Reed, M. D., & Yamamoto, K. H. (2012). A Straight Forward Guide for Processing Radiance and Reflectance for EO-1 ALI, Landsat 5 TM, Landsat 7 ETM+, and ASTER, 8. Retrieved from http://cegis.usgs.gov/soil_moisture/pdf/A Straight Forward guide for Processing Radiance and Reflectance_V_24Jul12.pdf

Fisher, J., Stratford, C. J., & Buckton, S. (2009). Variation in nutrient removal in three wetland blocks in relation to vegetation composition, inflow nutrient concentration and hydraulic loading. *Ecological Engineering*, *35*(10), 1387–1394. doi:10.1016/j.ecoleng.2009.05.009

Frohn, R. C., Reif, M., Lane, C., & Autrey, B. (2009). Satellite remote sensing of isolated wetlands using object-oriented classification of Landsat-7 data. *Wetlands*. doi:10.1672/08-194.1

Gao, X., Huete, A. R., Ni, W., & Miura, T. (2000). Optical-biophysical relationships of vegetation spectra without background contamination. *Remote Sensing of Environment*, *74*(00), 609–620. doi:10.1016/S0034-4257(00)00150-4

Gundogdu, K. S., & Guney, I. (2007). Spatial analyses of groundwater levels using universal kriging. *Journal of Earth System Science*, *116*(1), 49–55. doi:10.1007/s12040-007-0006-6

Gutierres, F. (2012). *Requirements for monitoring and assessment of the conservation status of Natura 2000 habitat types Aamsveen , Wittveen , Overijssel Province , The Netherlands* (p. 37). Enschede, the Netherlands.

Huete, a, Didan, K., Miura, T., Rodriguez, E. ., Gao, X., & Ferreira, L. . (2002). Overview of the radiometric and biophysical performance of the MODIS vegetation indices. *Remote Sensing of Environment*, *83*(1-2), 195–213. doi:10.1016/S0034-4257(02)00096-2

Interpolation - Wikipedia, the free encyclopedia. (n.d.). Retrieved February 03, 2015, from http://en.wikipedia.org/wiki/Interpolation#Polynomial_interpolation

Jacob, A. L., Bonnell, T. R., Dowhaniuk, N., & Hartter, J. (2014). Topographic and spectral data resolve land cover misclassification to distinguish and monitor wetlands in western Uganda. *ISPRS Journal of Photogrammetry and Remote Sensing*, *94*, 114–126. doi:10.1016/j.isprsjprs.2014.05.001

Katz, R. W., Parlange, M. B., & Naveau, P. (2002). Statistics of extremes in hydrology. *Advances in Water Resources*, *25*, 1287–1304. doi:10.1016/S0309-1708(02)00056-8

Kotchenova, S. Y., & Vermote, E. F. (2007). Validation of a vector version of the 6S radiative transfer code for atmospheric correction of satellite data. Part II. Homogeneous Lambertian and anisotropic surfaces. *Applied Optics*, *46*, 4455–4464. doi:10.1364/AO.46.004455

Lamers, L. P. M., Smolders, A. J. P., & Roelofs, J. G. M. (2002). The restoration of fens in the Netherlands. *Hydrobiologia*, *478*(1-3), 107–130. doi:10.1023/A:1021022529475

Loiselle, S., Bracchini, L., Bonechi, C., & Rossi, C. (2001). Modelling energy fluxes in remote wetland ecosystems with the help of remote sensing. *Ecological Modelling*, *145*, 243–261. doi:10.1016/S0304-3800(01)00394-5

Malekmohammadi, B., & Rahimi Blouchi, L. (2014). Ecological risk assessment of wetland ecosystems using Multi Criteria Decision Making and Geographic Information System. *Ecological Indicators*, *41*, 133–144. doi:10.1016/j.ecolind.2014.01.038

Martínez-López, J., Carreño, M. F., Palazón-Ferrando, J. a., Martínez-Fernández, J., & Esteve, M. a. (2014). Remote sensing of plant communities as a tool for assessing the condition of semiarid Mediterranean saline wetlands in agricultural catchments. *International Journal of Applied Earth Observation and Geoinformation*, *26*, 193–204. doi:10.1016/j.jag.2013.07.005

Oasmaa, a, Elliott, D. C., & Mu, S. (2009). Quality Control in Fast Pyrolysis Bio-Oil Production and Use. *Environmental Progress*, *28*(2), 404–409. doi:10.1002/ep

Ozesmi, S. L., & Bauer, M. E. (2002). Satellite remote sensing of wetlands. *Wetlands Ecology and Management*, *10*, 381–402. doi:10.1023/A:1020908432489

Proud, S. R., Rasmussen, M. O., Fensholt, R., Sandholt, I., Shisanya, C., Mutero, W., … Anyamba, A. (2010). Improving the SMAC atmospheric correction code by analysis of Meteosat Second Generation NDVI and surface reflectance data. *Remote Sensing of Environment*, *114*(8), 1687–1698. doi:10.1016/j.rse.2010.02.020

Seibert, J., Bishop, K., Rodhe, A., & McDonnell, J. J. (2003). Groundwater dynamics along a hillslope: A test of the steady state hypothesis. *Water Resources Research*, *39*(1), n/a–n/a. doi:10.1029/2002WR001404

Siciliano, D., Wasson, K., Potts, D. C., & Olsen, R. C. (2008). Evaluating hyperspectral imaging of wetland vegetation as a tool for detecting estuarine nutrient enrichment. *Remote Sensing of Environment*, *112*(11), 4020–4033. doi:10.1016/j.rse.2008.05.019

Sluiter, R. (2009). *Interpolation methods for climate data*. Retrieved from https://www.snap.uaf.edu/sites/default/files/files/Interpolation_methods_for_climate_data.pdf

Sorana-Daniela, B. (2006). Pearson versus Spearman, Kendall's Tau Correlation Analysis on Structure-Activity Relationships of Biologic Active Compounds from Leonardo Journal of Sciences. Retrieved from http://ljs.academicdirect.org/A09/179_200.htm

The Yale Center for Earth. (2010). *ASTER Images*. *Earth* (pp. 1–6).

Tweed, S. O., Leblanc, M., Webb, J. a., & Lubczynski, M. W. (2006). Remote sensing and GIS for mapping groundwater recharge and discharge areas in salinity prone catchments, southeastern Australia. *Hydrogeology Journal*, *15*(1), 75–96. doi:10.1007/s10040-006-0129-x

Vermote, E. F., Tanré, D., Deuzé, J. L., Herman, M., & Morcrette, J. J. (1997). Second simulation of the satellite signal in the solar spectrum, 6s: an overview. *IEEE Transactions on Geoscience and Remote Sensing*, *35*(3), 675–686. doi:10.1109/36.581987

Wang, C.-Y., Sample, D. J., Day, S. D., & Grizzard, T. J. (2014). Floating treatment wetland nutrient removal through vegetation harvest and observations from a field study. *Ecological Engineering*, 1–12. doi:10.1016/j.ecoleng.2014.05.018

Wang, J., Rich, P. M., & Price, K. P. (2003). Temporal responses of NDVI to precipitation and temperature in the central Great Plains, USA. *International Journal of Remote Sensing*, *24*(February 2015), 2345–2364. doi:10.1080/01431160210154812

Water Resource Characterization DSS - Phosphorus. (n.d.). Retrieved February 11, 2015, from http://www.water.ncsu.edu/watershedss/info/phos.html

Wikipedia. (2014). Aamsveen - Wikipedia. Retrieved August 10, 2014, from http://nl.wikipedia.org/wiki/Aamsveen

Zomer, R. J., Trabucco, a, & Ustin, S. L. (2009). Building spectral libraries for wetlands land cover classification and hyperspectral remote sensing. *Journal of Environmental Management*, *90*(7), 2170–7. doi:10.1016/j.jenvman.2007.06.028

Zorrilla-Miras, P., Palomo, I., Gómez-Baggethun, E., Martín-López, B., Lomas, P. L., & Montes, C. (2014). Effects of land-use change on wetland ecosystem services: A case study in the Doñana marshes (SW Spain). *Landscape and Urban Planning*, *122*, 160–174. doi:10.1016/j.landurbplan.2013.09.013

APPENDIX A

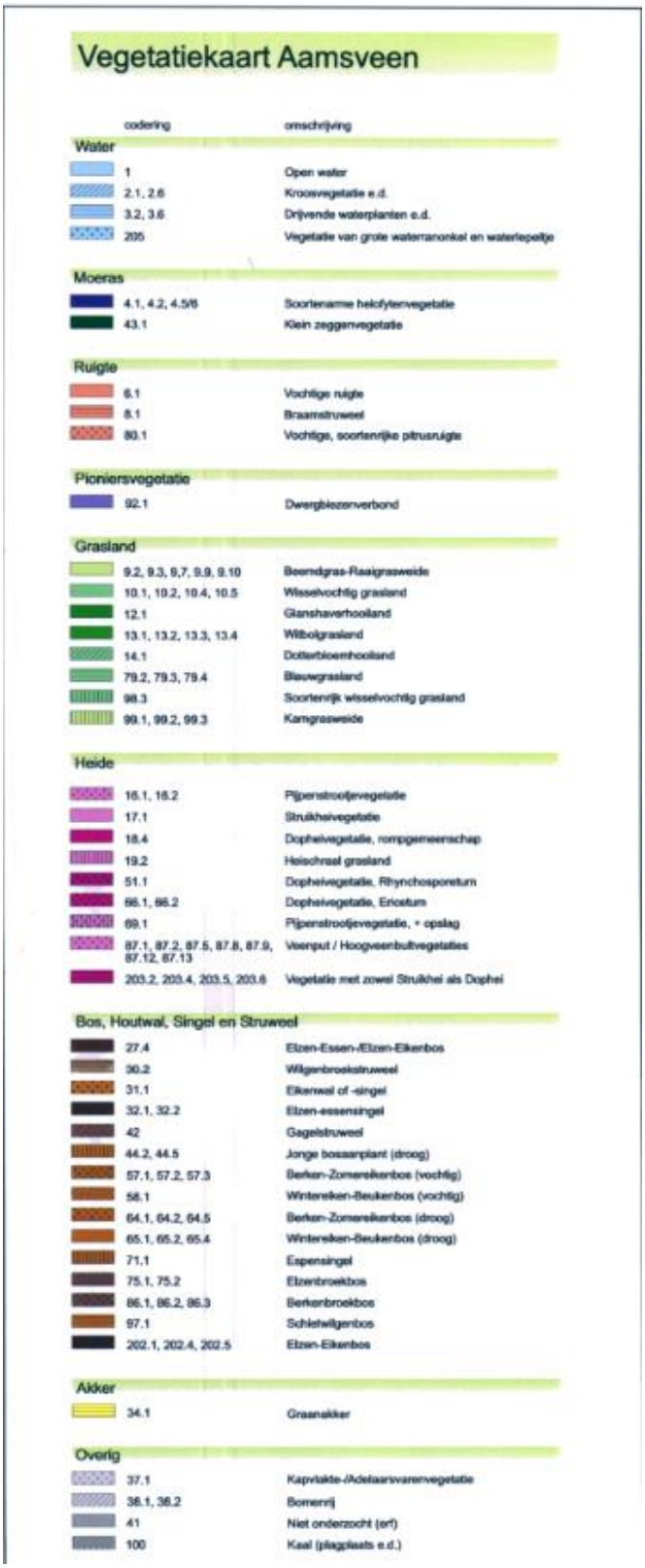
Vegetatiekaart Aamsveen
codering
omschrijving
Water
1
Open water
2.1, 2.6
Kroosvegetatie e.d.
3.2, 3.6
Drijvende waterplanten e.d.
205
Vegetatie van grote waterranonkel en waterlepeltje
Moeras
4.1, 4.2, 4.5/6
Soortenarme helofytenvegetatie
43.1
Klein zeggenvegetatie
Ruigte
6.1
Vochtige ruigte
8.1
Braamstruweel
80.1
Vochtige, soortenrijke pitrusruigte
Pioniersvegetatie
92.1
Dwergbiezenverbond
Grasland
9.2, 9.3, 9,7, 9.9, 9.10
Beemdgras-Raaigrasweide
10.1, 10.2, 10.4, 10.5
Wisselvochtig grasland
12.1
Glanshaverhooiland
13.1, 13.2, 13.3, 13.4
Wilbolgrasland
14.1
Dotterbloemhooiland
79.2, 79.3, 79.4
Blauwgrasland
98.3
Soortenrijk wisselvochtig grasland
99.1, 99.2, 99.3
Kamgrasweide
Heide
16.1, 16.2
Pijpenstrootjevegetatie
17.1
Struikheivegetatie
18.4
Dopheivegetatie, rompgemeenschap
19.2
Heischraal grasland
51.1
Dopheivegetatie, Rhynchosporetum
86.1, 86.2
Dopheivegetatie, Ericetum
69.1
Pijpenstrootjevegetatie, + opslag
87.1, 87.2, 87.5, 87.8, 87.9, 87.12, 87.13
Veenput / Hoogveenbultvegetaties
203.2, 203.4, 203.5, 203.6
Vegetatie met zowel Struikhei als Dophei
Bos, Houtwal, Singel en Struweel
27.4
Elzen-Essen-/Elzen-Eikenbos
30.2
Wilgenbroekstruweel
31.1
Eikenwal of -singel
32.1, 32.2
Elzen-essensingel
42
Gagelstruweel
44.2, 44.5
Jonge bossanplant (droog)
57.1, 57.2, 57.3
Berken-Zomereikenbos (vochtig)
58.1
Wintereiken-Beukenbos (vochtig)
64.1, 64.2, 64.5
Berken-Zomereikenbos (droog)
65.1, 65.2, 65.4
Wintereiken-Beukenbos (droog)
71.1
Espensingel
75.1, 75.2
Elzenbroekbos
86.1, 86.2, 86.3
Berkenbroekbos
97.1
Schietwilgenbos
202.1, 202.4, 202.5
Elzen-Eikenbos
Akker
34.1
Graanakker
Overig
37.1
Kapvlakte-/Adelaarsvarenvegetatie
38.1, 38.2
Bomenrij
41
Niet onderzocht (erf)
100
Kaal (plaggkaats e.d.)

APPENDIX B

	Code	Vegetation type
Open water		
	50A-1	Open water
Watervegetaties		
	05-1	Type van fonteinkruiden met drijvende bladeren.
Zure vennen		
	06-1	Type van Knolrus
	06-2	Type van Knolrus
	06-3	Type van Veelstengelige waterbies
Overige vennen		
	06-4	Type van Duizendknoopfonteinkruid
	06C2-1	Type van Vlottende bies
Moerasvegetaties		
	08-1	Type van rietfacies
	08B3-1	Type van Riet met zure soorten
	08B3-2	Type van Riet met zure soorten
	32-1	Type van Riet met slechts een enkel ruigtkruid
	32-2	Type van Riet met slechts een enkel ruigtkruid
Kleine zeggenvegetaties		
	09-1	Natte Pitrusruigten
	09-2	Type van Zwarte zegge en Moerasstruisgras
	09-3	Type van Zwarte zegge en Moerasstruisgras
	09-4	Type van Snavelzegge
	09A-1	Type van Zwarte zegge en Moerasstruisgras
	09A-2	Type van Zwarte zegge en Moerasstruisgras
	09A-3	Type van Zwarte zegge en Moerasstruisgras
Hoogveenslenkgemeenschappen		
	10-1	Type van Waterveenmos
	10-2	Type van Waterveenmos
	10-3	Type van Waterveenmos
	10-4	Type van Waterveenmos
	10-5	Type van Waterveenmos
	10A2-1	Type van Witte snavelbies en/of Ronde zonnedauw
Eenarig wollegrasslenkgemeenschappen		
	10-6	Type van Eenarig wollegras
Pijpenstrovegetaties		
	11-1	Type van Pijpenstrootje
	11-6	Type van Pijpenstrootje
Pijpenstrovegetaties met veenmossen		
	11-2	Type van Pijpenstrootje
	11-3	Type van Pijpenstrootje
Natte heiden		
	11-4	Type van Wilde gagel, en Sporkehout en/of Zachte berk

	11-5	Type van Wilde gagel, en Sporkehout en/of Zachte berk
	11A-1	Type van Gewone dophei
	11A2-1	Type van Gewone dophei
	11A2-2	Type van Gewone dophei
	11A2-3	Type van Gewone dophei
Snavelbiesgemeenschappen		
	11A1-1	Type van snavelbiezen en Kleine zonnedauw
	11A1-2	Type van snavelbiezen en Kleine zonnedauw
Natte heiden met hoogveensoorten		
	11-7	Type van Eenarig wollegras en Gewone dophei
	11A2-4	Type van Gewone dophei
Hoogveengemeenschappen		
	11A2-5	Type van Lavendelhei en Gewone dophei
	11B-1	Type van Kleine veenbes
Overstromingsgraslanden		
	12B-1	Type van Fioringras
	12B1-1	Type van Fioringras en hooilandsoorten
	12B-2	Type van Fioringras en hooilandsoorten
	12B-3	Type van Fioringras en hooilandsoorten
	12B-4	Type van Fioringras en natte soorten
	12B-5	Type van Fioringras en zure soorten
	12B-6	Type van Fioringras en zure soorten
	12B-7	Type van Mannagras
	16-1	Type van Gestreepte witbol
	16-2	Type van Gestreepte witbol
	16-3	Type van Gewoon reukgras, Gewoon struisgras en Rood zwenkgra
	16-4	Type van Gewoon reukgras, Gewoon struisgras en Rood zwenkgra
	16-5	Type van Gewoon reukgras, Gewoon struisgras en Rood zwenkgra
	16-6	Type van Gewoon reukgras, Gewoon struisgras en Rood zwenkgra
	16A-1	Type van Veldrus
Schraallanden		
	16A-2	Type van Zwarte zegge en Moerasstruisgras met schrale soorte
	16A-3	Type van Pijpenstrootje
	16A-4	Type van Pijpenstrootje
	16A-5	Type van Pijpenstrootje en Blauwe knoop
	16A-6	Type van Pijpenstrootje en Blauwe zegge
	16A-7	Type van Pijpenstrootje en Blauwe zegge
	18-1	Type van Adelaarsvaren
	19A2-1	Type van Heidekartelblad en/of Klokjesgentiaan
Struikheiden		

	20A1-1	Type van Struikhei
	20A1-2	Type van Struikhei
	20A2-1	Type van Struikhei
Ruigten		
	33-1	Type van Grote brandnetel en Akkerdistel
Struwelen		
	36A-1	Type van Wilde gagel en Grauwe wilg
	36A1-1	Type van Geoorde wilg
	36A-2	Type van Sporkehout
	36A2-1	Type van Grauwe wilg
	36A2-2	Type van Grauwe wilg
	36A2-3	Type van Grauwe wilg
Elzenbroekbos		
	39A-1	Degradatietypen met Zwarte els
	39A-2	Degradatietypen met Zwarte els
	39A-3	Degradatietypen met Zwarte els
	39A-4	Degradatietypen met Zwarte els
	39A-5	Degradatietypen met Zwarte els
	39A1-1	Type van Elzenzegge, IJle zegge en Zwarte bes
Berkenbroekbos		
	40A-1	Type van Zachte berk en Veenmossen
	40A-2	Type van Zachte berk
	40A-3	Type van Zachte berk en Veenmossen
	40A-4	Type van Zachte berk
	40A-5	Type van Zachte berk
Bossen van armere gronden		
	41A3-2	Type van Dophei en/of Struikhei
	42-1	Degradatietypen van Eiken-Berkenbos en Eiken-Beukenbos
	42-2	Degradatietypen van Eiken-Berkenbos en Eiken-Beukenbos
	42-3	Type van bramen
	42-4	Type van eik en els
	42A-1	Degradatietypen van Eiken-Berkenbos en Eiken-Beukenbos
	42A1-1	Type van berk en eik
	42A1-2	Type van berk en eik
	42A-2	Degradatietypen van Eiken-Berkenbos en Eiken-Beukenbos
	42A2-1	Type van Beuk en eik
	42A2-	Type van Beuk en eik

	2	
	42A2-3	Type van Beuk en eik
	42A2-4	Type van Beuk en eik
	42A2-5	Type van eik en els
	42A2-6	Type van eik en els
Bossen van rijkere gronden		
	43-1	Degradatietypen van Essen- Iepen-en Haagbeukenbossen
	43-2	Degradatietypen van Essen- Iepen-en Haagbeukenbossen
	43B2-1	Type van Gewone es en Vogelkers
	43C1-1	Type van Haagbeuk
Type van kale bodem		
	50C-1	Type van kale bodem
Erven, paden, parkeerplaatsen		
	300-1	Erven, paden, parkeerplaatsen

APPENDIX C

Year	precipitation	evaporation	Pre.-Eva.
1995	766.7	589.7	177
1996	623.9	520.7	103.2
1997	713.2	567.1	146.1
1998	1012.7	485.2	527.5
1999	836.5	580.1	256.4
2000	847.9	531.3	316.6
2001	831.9	556.7	275.2
2002	777.3	551.4	225.9
2003	616.6	642.4	-25.8
2004	851.3	565.6	285.7
2005	797	590.7	206.3
2006	720.7	595.4	125.3
2007	915.5	565.5	350
2008	727.1	579.9	147.2
2009	776.3	604.6	171.7
2010	789.5	577	212.5
2011	642.9	581.5	61.4
2012	756.6	571.6	185
2013	751.6	558.7	192.9